

# **Observation of noise in production VPTs at 1.8T**

## **Addendum: details of observed noisy behaviour.**

B W Kennedy

21 March 2003

### **1. INTRODUCTION**

A previous note [1] has described the observation of noisy behaviour consistent with electrical discharges in a sample of VPTs. This Addendum presents further details of the observations.

For each VPT, two plots are shown. Firstly the result of a standard set of measurements made in the RAL test rig [2], and secondly a display of the raw data illustrating the “spike” in the VPT output at a particular angle. In all cases the data were taken in a 1.8T magnetic field. . The measurements shown here are in raw ADC bins.

The “peak width” referred to in the figures is the Gaussian width of the sequence of 5000 measurements of VPT output at one angle. In normal operation these widths are typically 3-5 bins; an increase in width is often an indication of noise in the VPT output.

In this note, VPTs are always identified by their bar-code number.

### **2. DETAILS OF NOISE OBSERVATIONS**

## 2.1 VPT 790

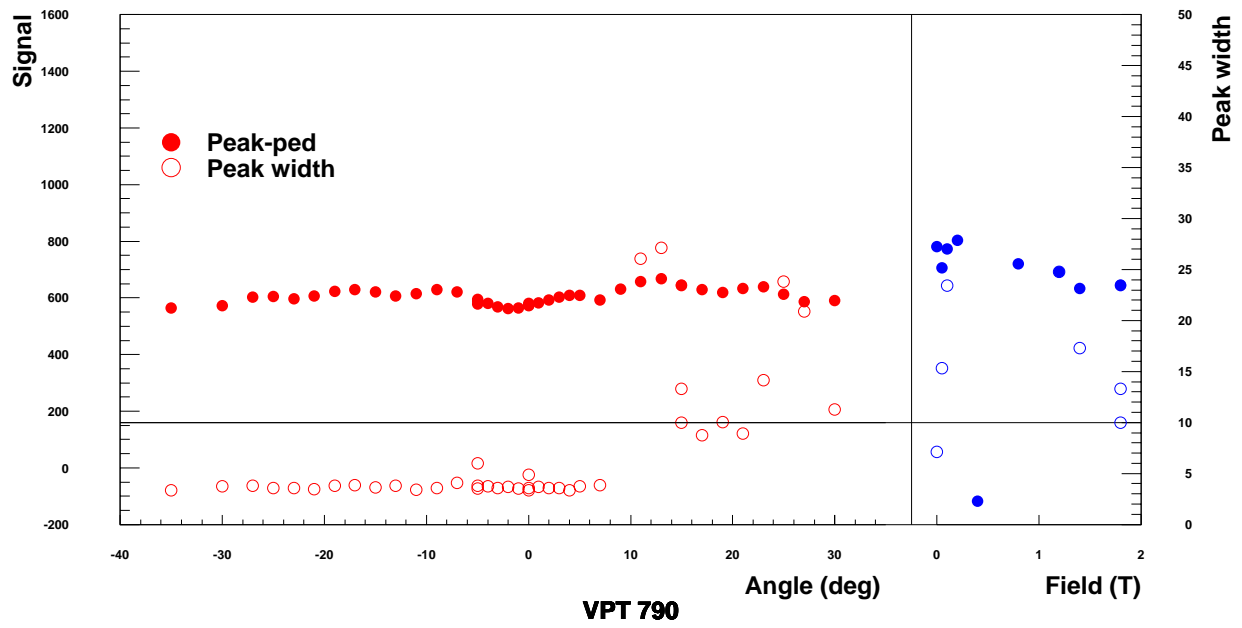


Figure 1. VPT 790 - Standard measurement sequence

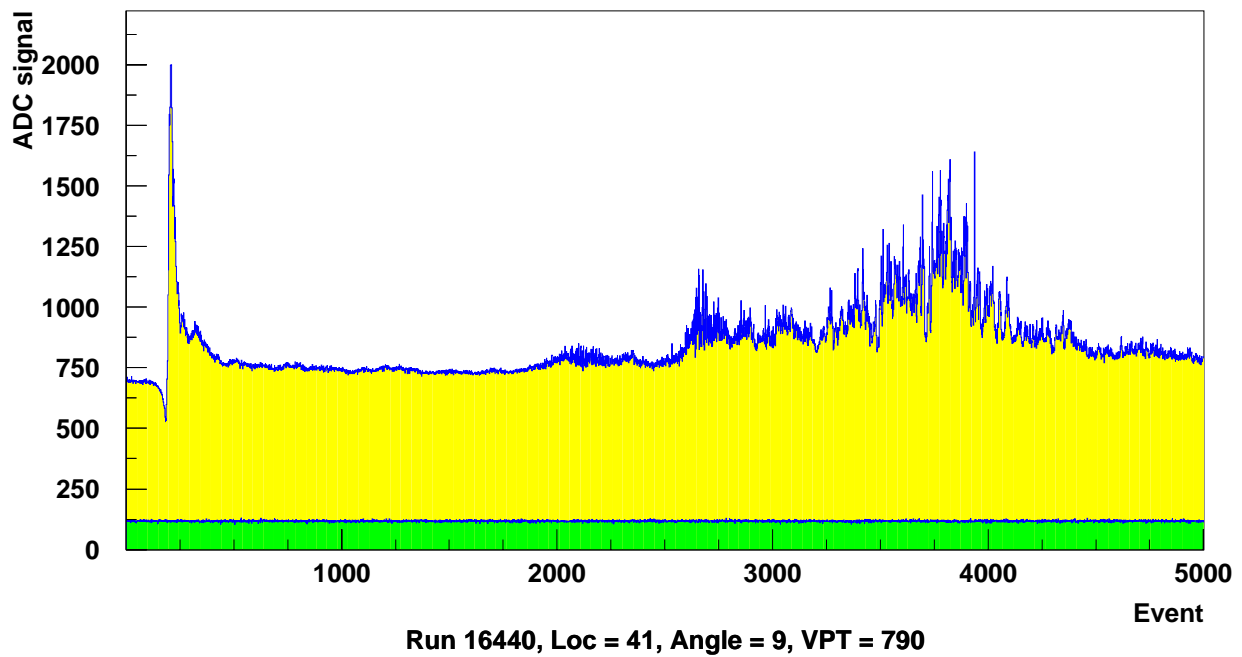


Figure 2. VPT 790 - raw data sequence at 9° to magnetic field

## 2.2 VPT 1503

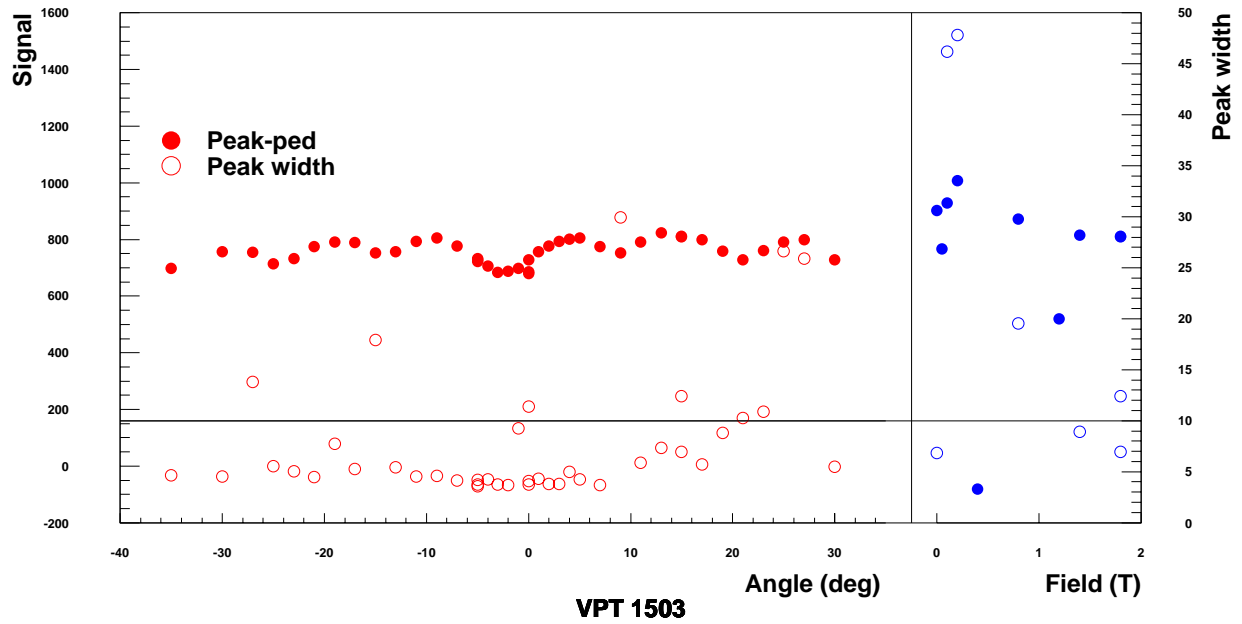
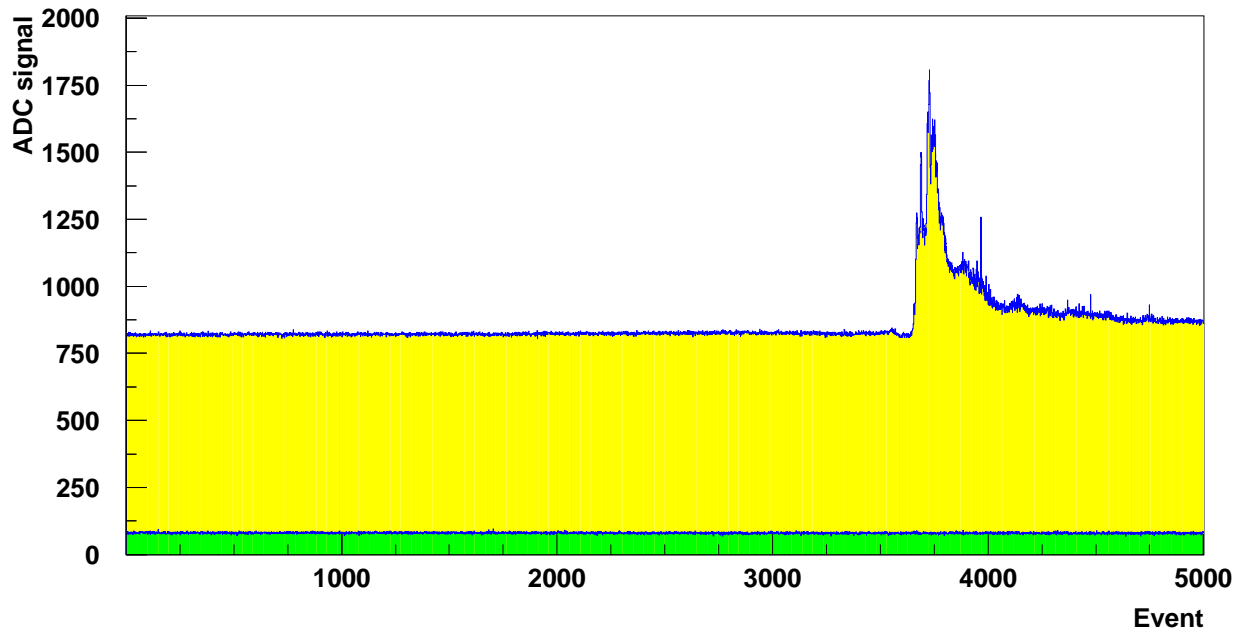


Figure 3. VPT 1503 - Standard measurement sequence



Run 16760, Loc = 35, Angle = 9, VPT = 1503

Figure 4. VPT 1503 - raw data sequence at 9° to magnetic field

### 2.3 VPT 1560

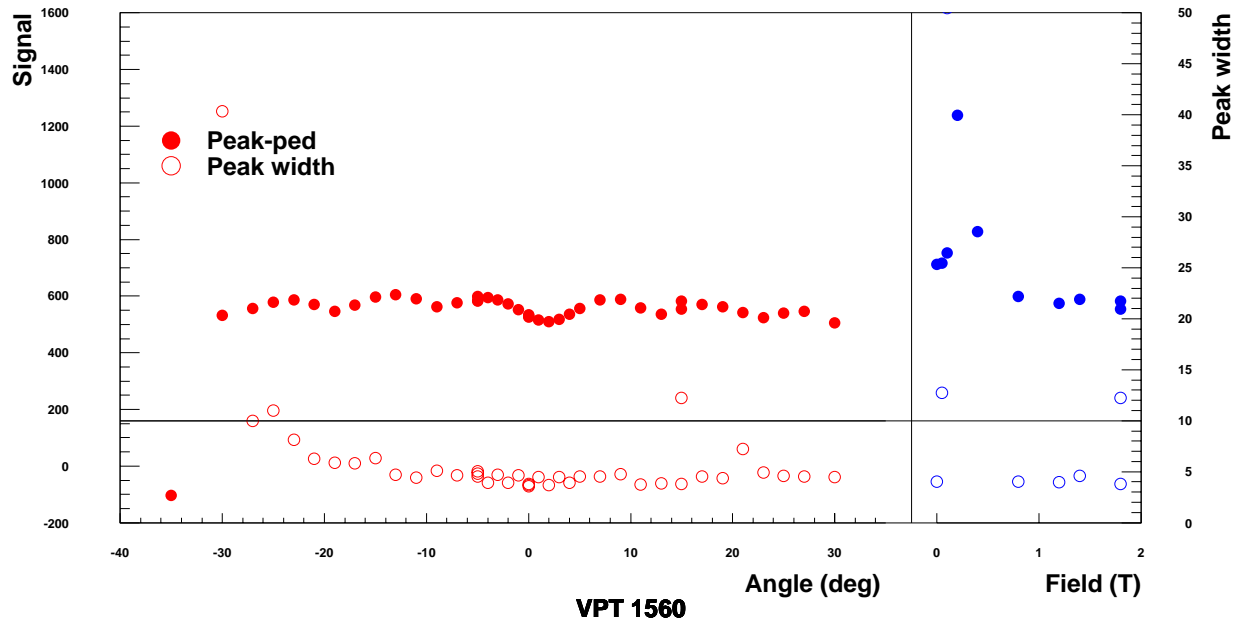


Figure 5. VPT 1560 - Standard measurement sequence

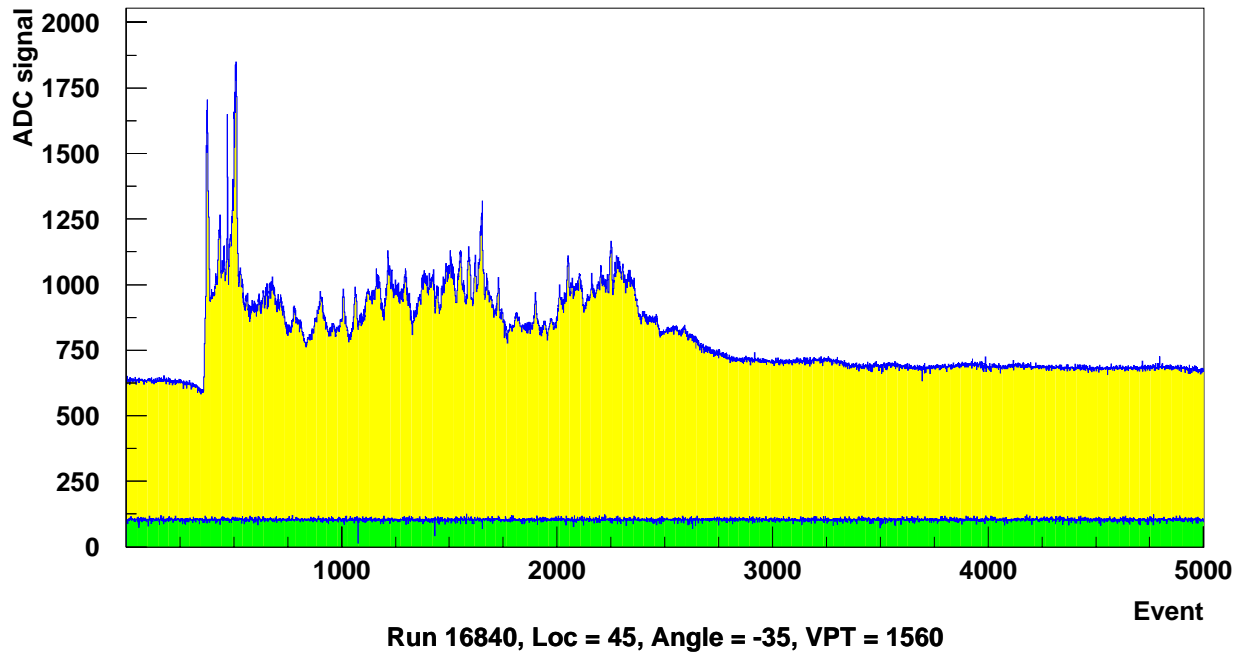


Figure 6. VPT 1560 - raw data sequence at  $-35^\circ$  to magnetic field

## 2.4 VPT 1638

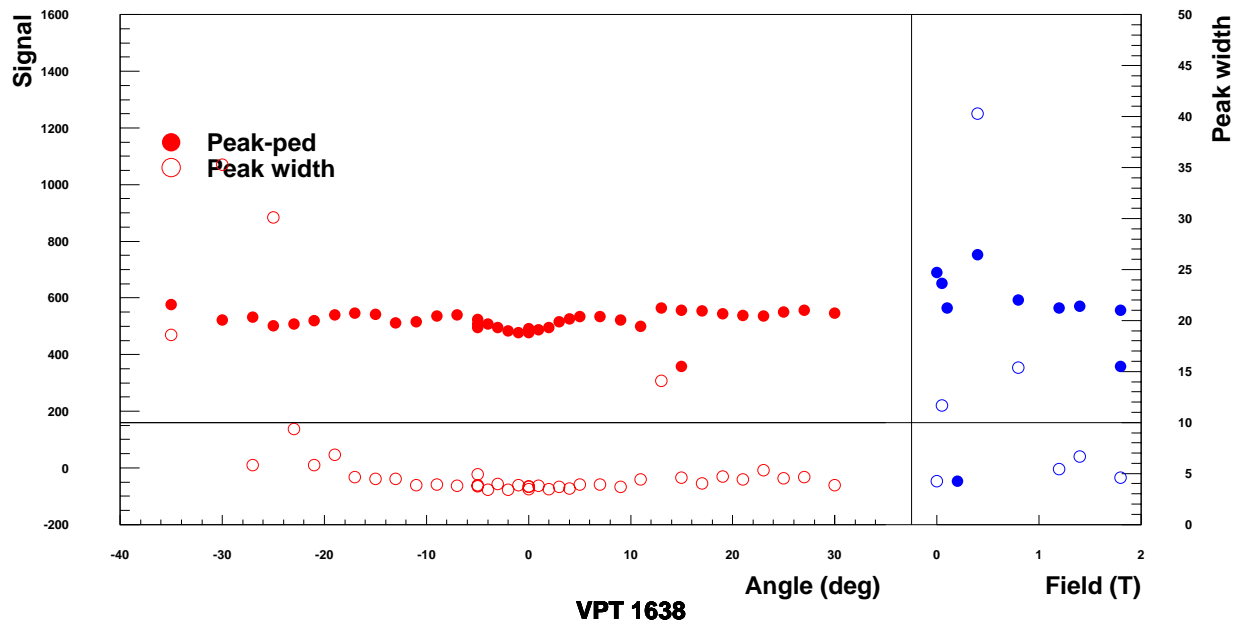


Figure 7. VPT 1638 - Standard measurement sequence

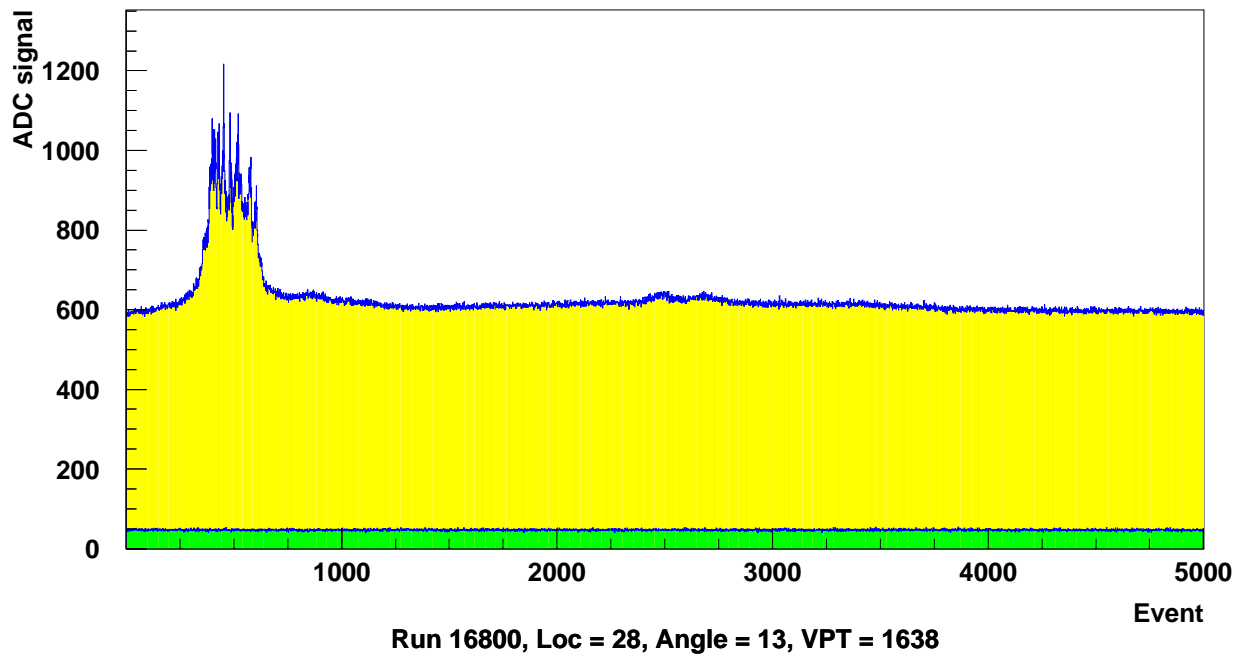


Figure 8. VPT 1638 - raw data sequence at 13° to magnetic field

## 2.5 VPT 1641

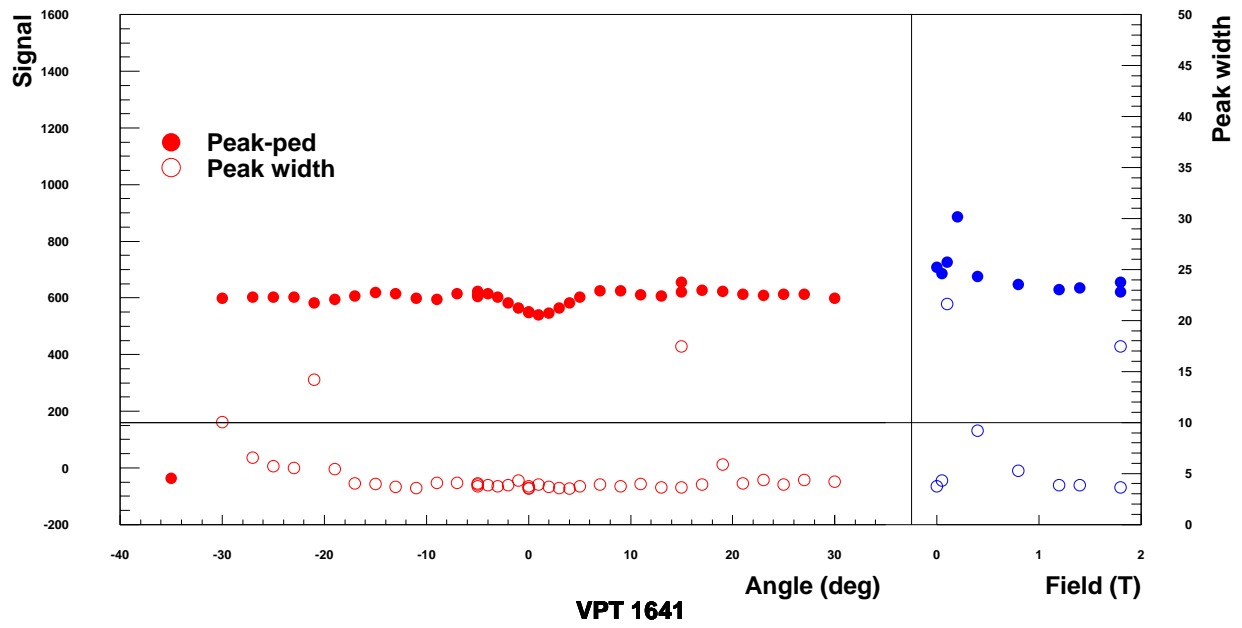


Figure 9. VPT 1641 - Standard measurement sequence

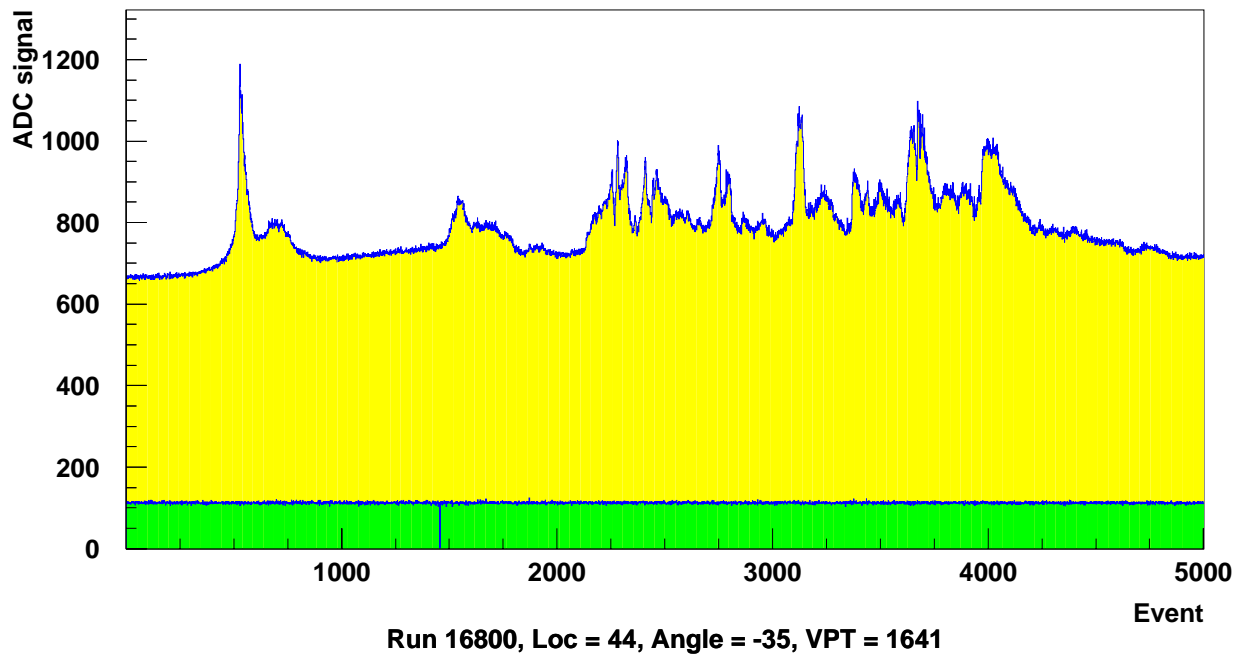


Figure 10. VPT 1641 - raw data sequence at  $-35^\circ$  to magnetic field

## 2.6 VPT 1700

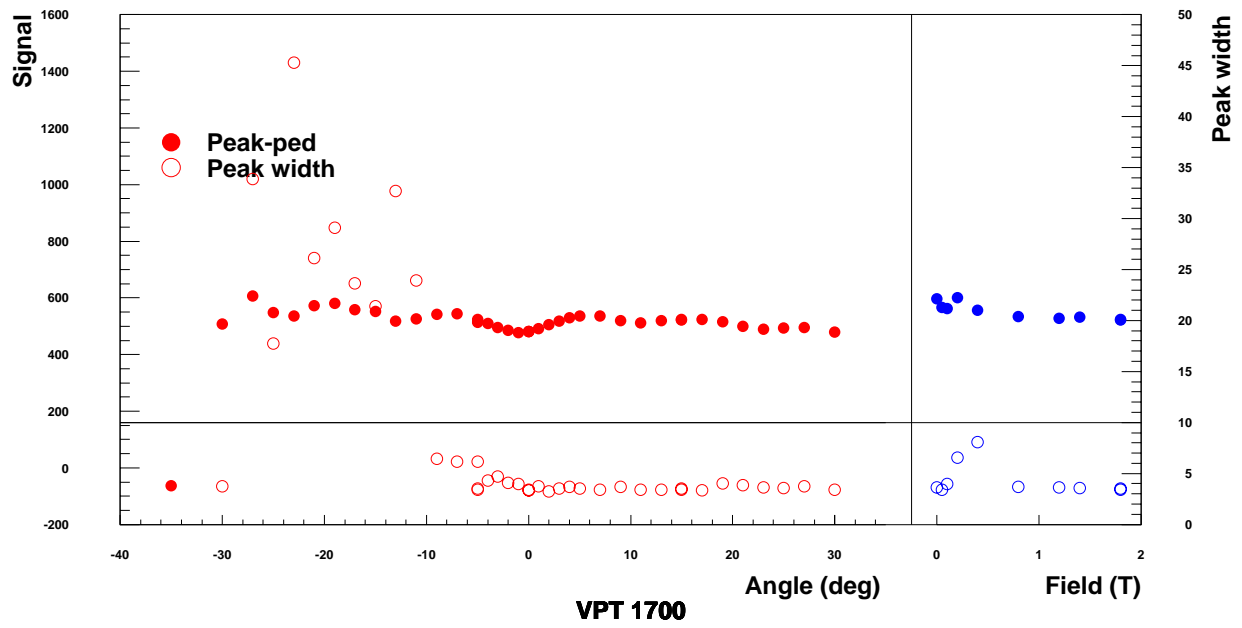


Figure 11. VPT 1700 - Standard measurement sequence

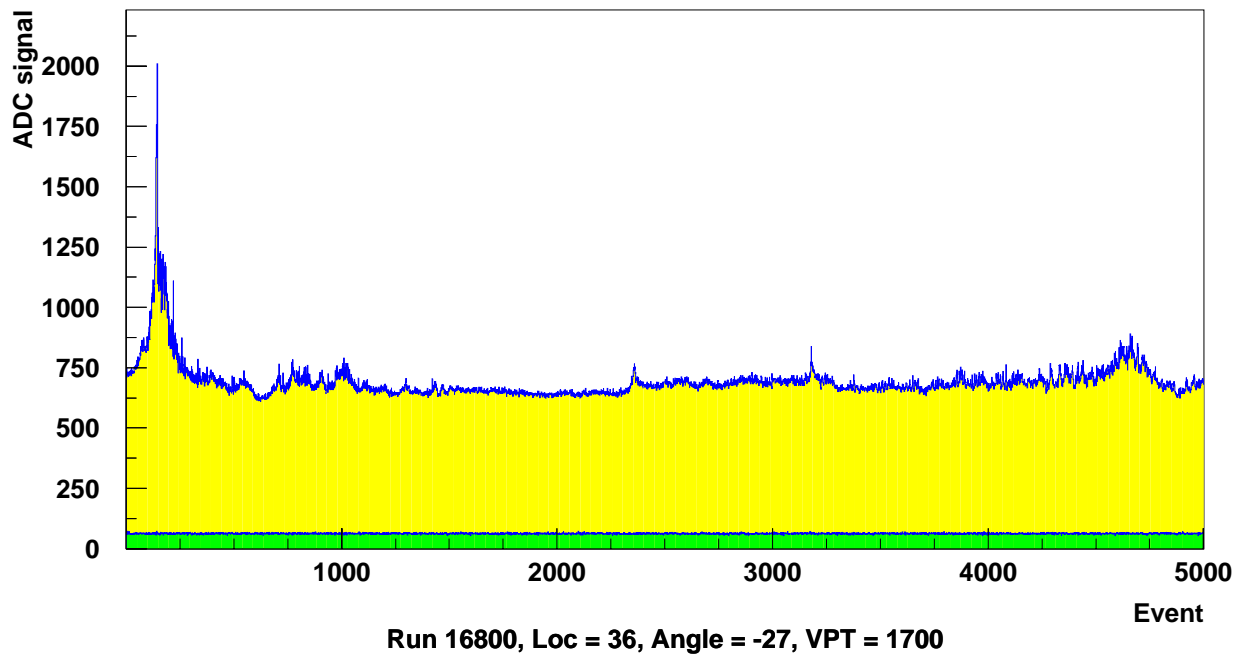


Figure 12. VPT 1700 - raw data sequence at  $-27^\circ$  to magnetic field

## 2.7 VPT 1742

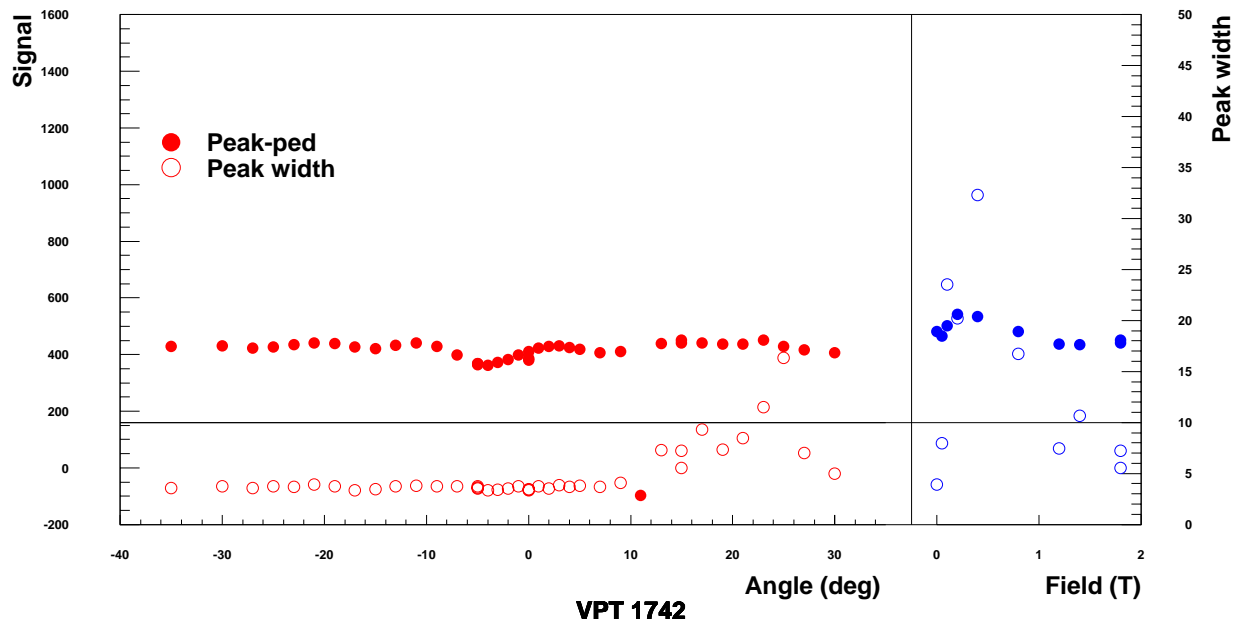


Figure 13. VPT 1742 - Standard measurement sequence

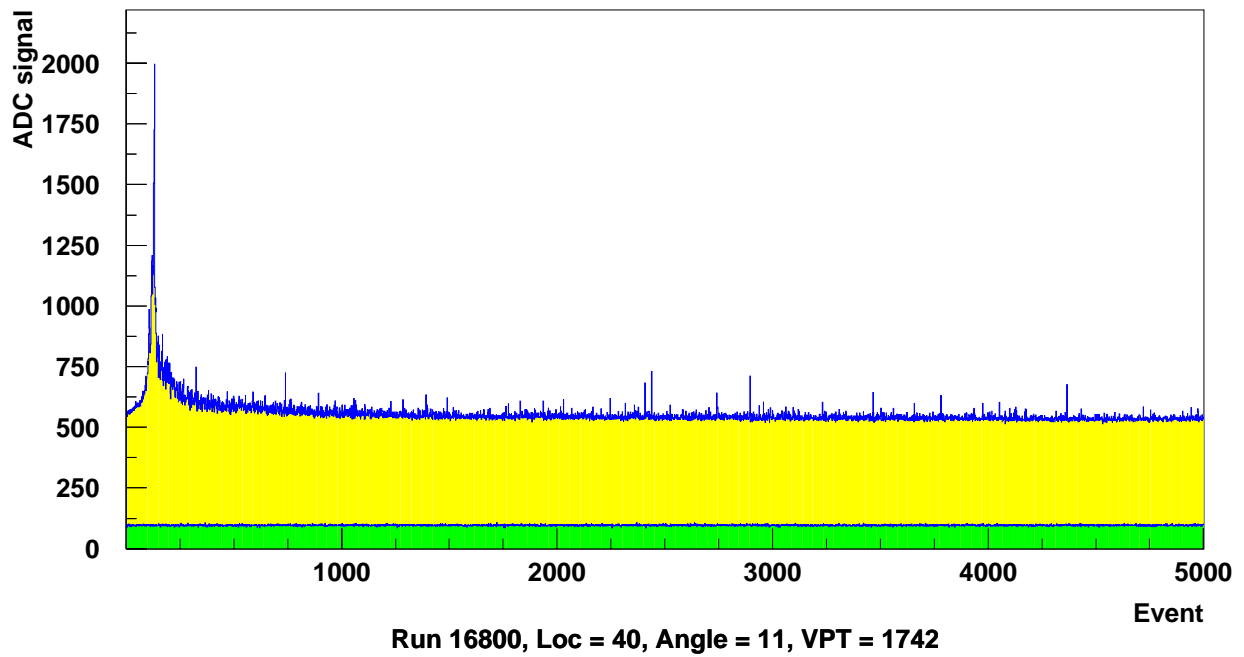


Figure 14. VPT 1742 - raw data sequence at 11° to magnetic field

## 2.8 VPT 1981

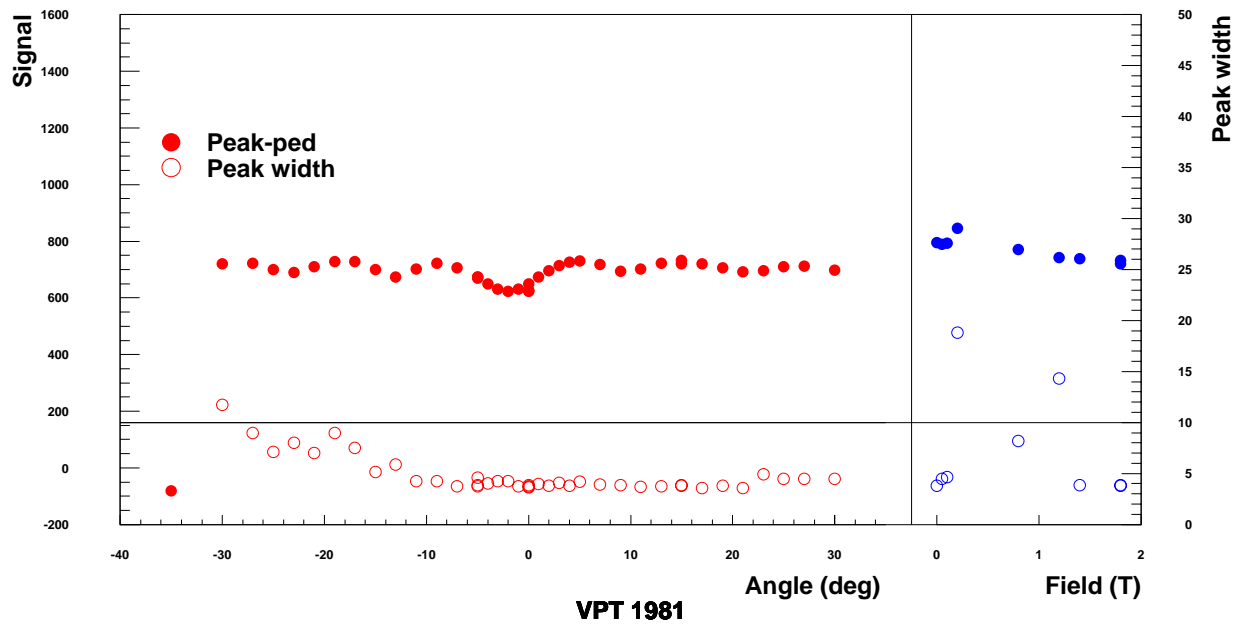


Figure 15. VPT 1981 - Standard measurement sequence

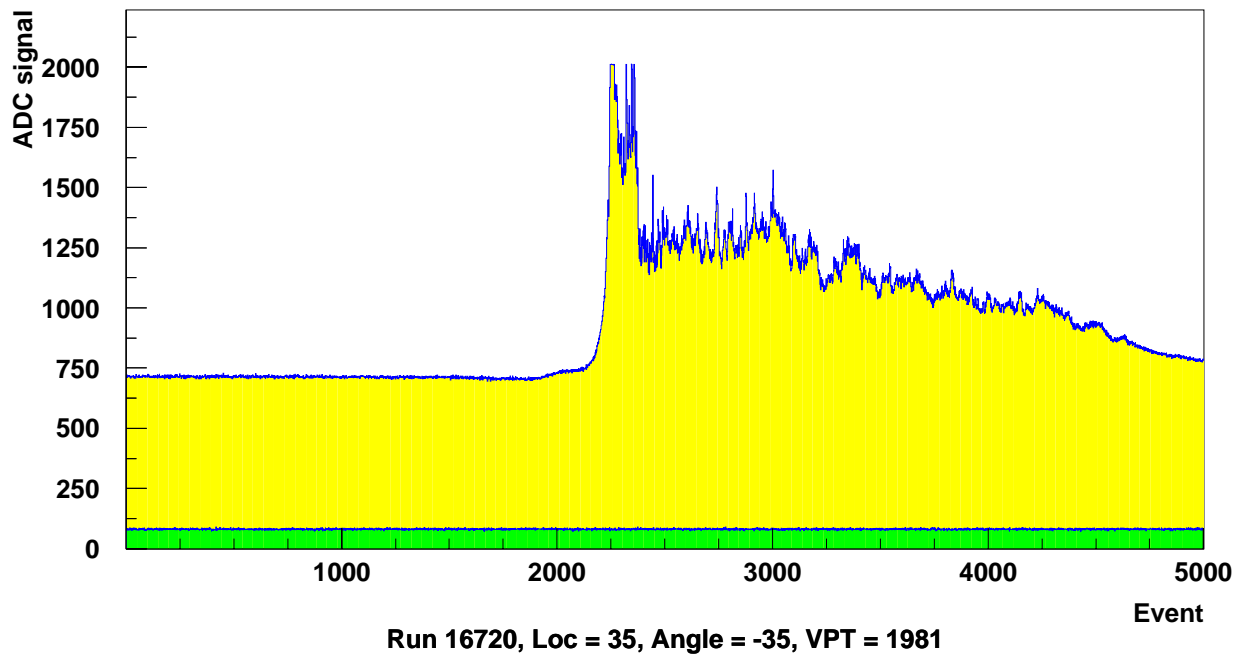


Figure 16. VPT 1981 - raw data sequence at  $-35^\circ$  to magnetic field

## 2.9 VPT 2020

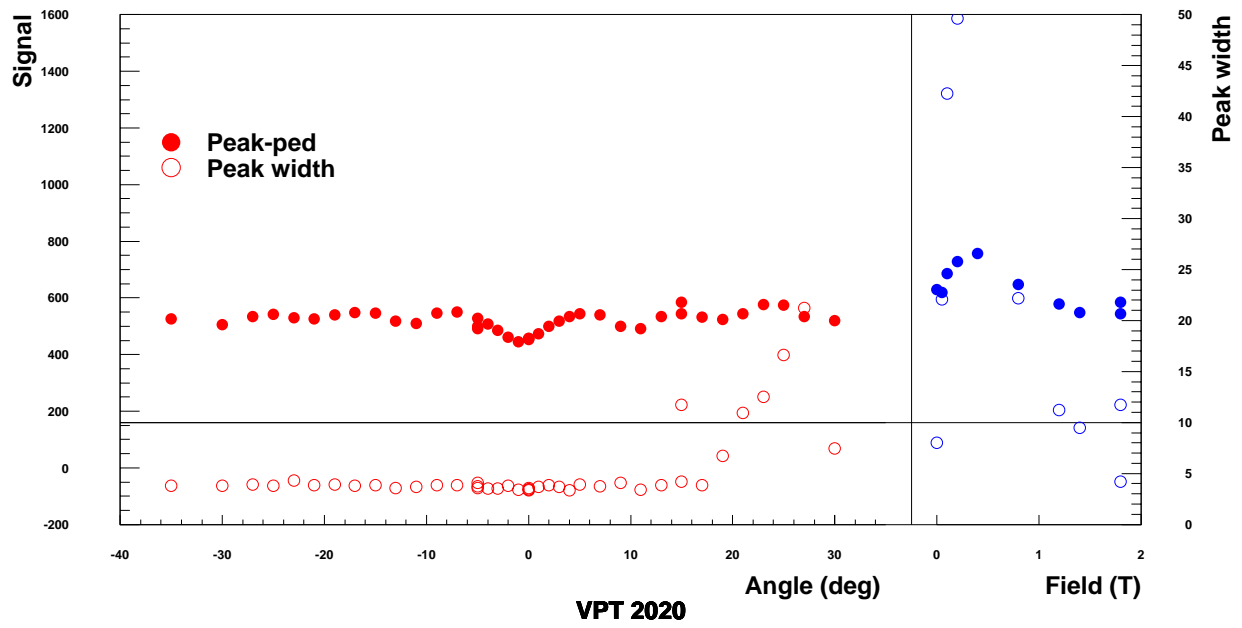


Figure 17. VPT 2020 - Standard measurement sequence

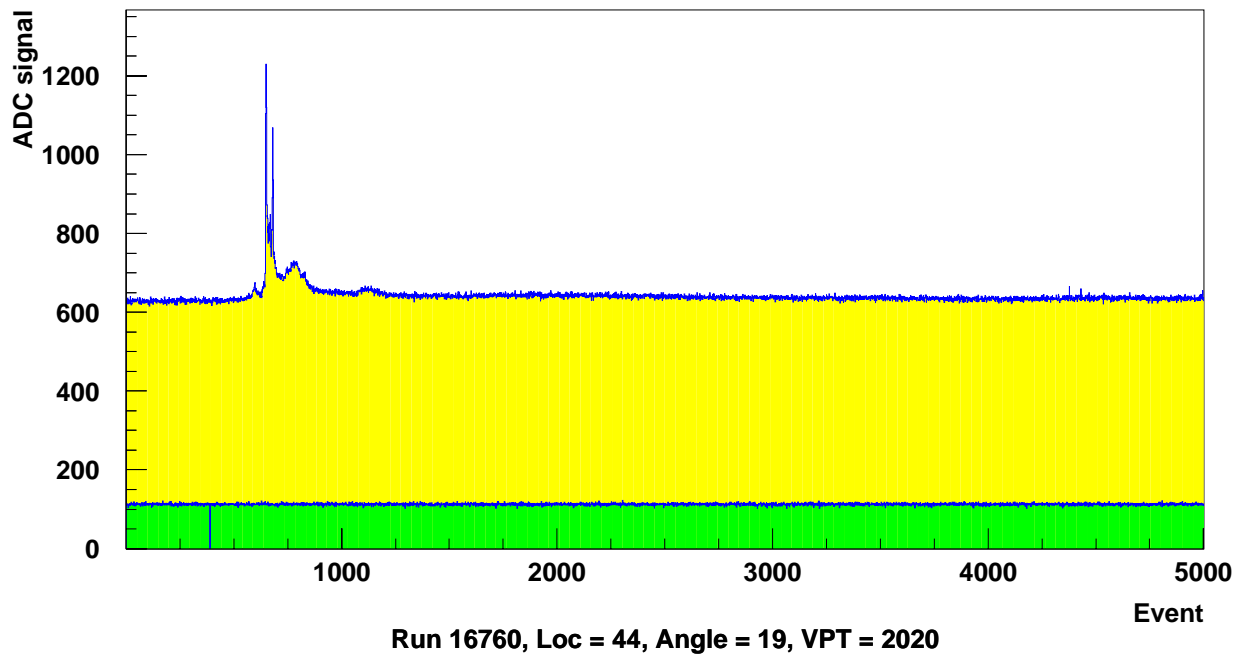


Figure 18. VPT 2020 - raw data sequence at 19° to magnetic field

## 2.10 VPT 2036

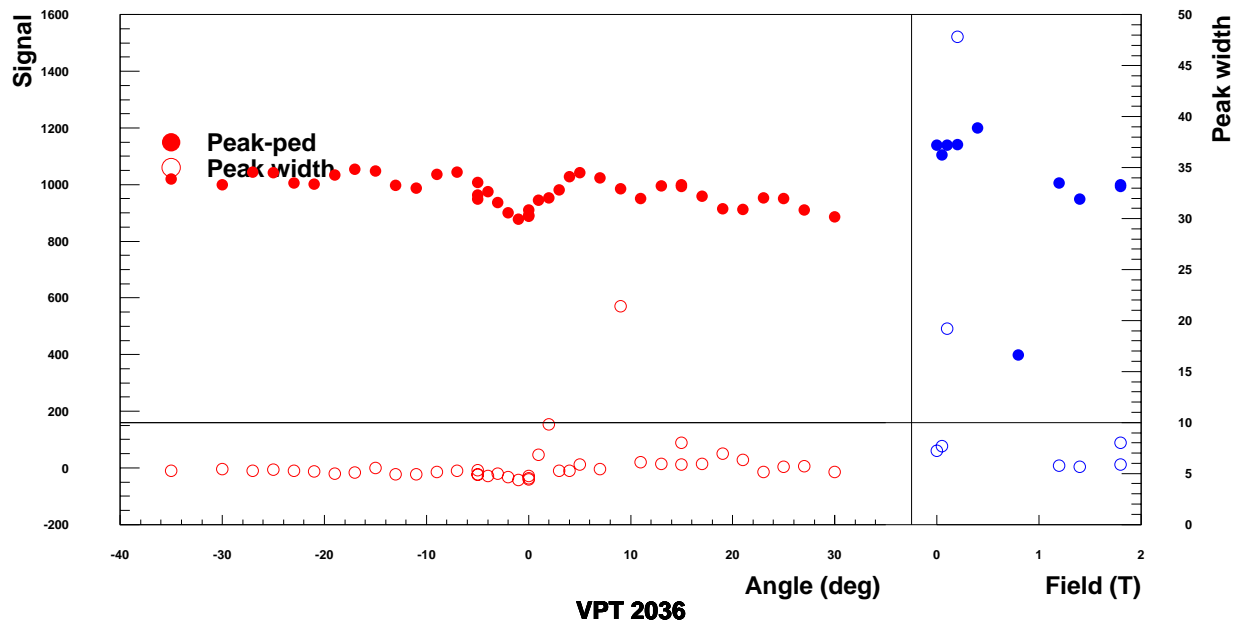


Figure 19. VPT 2036 - Standard measurement sequence

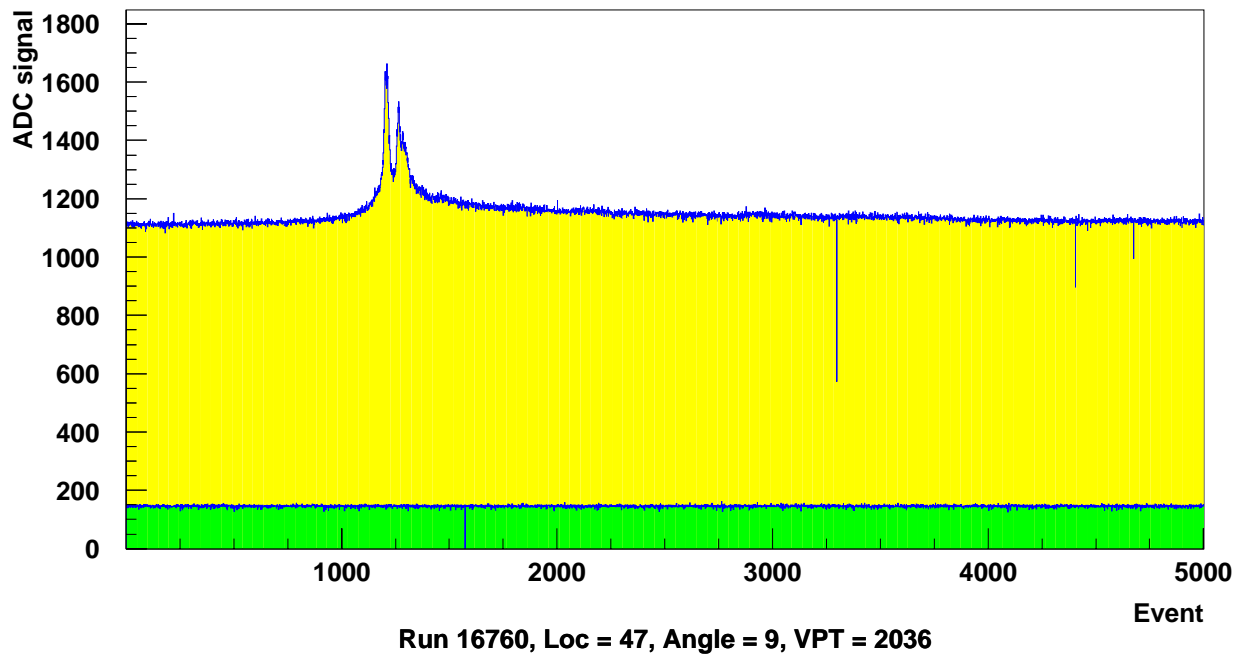


Figure 20. VPT 2036 - raw data sequence at 9° to magnetic field

## 2.11 VPT 2105

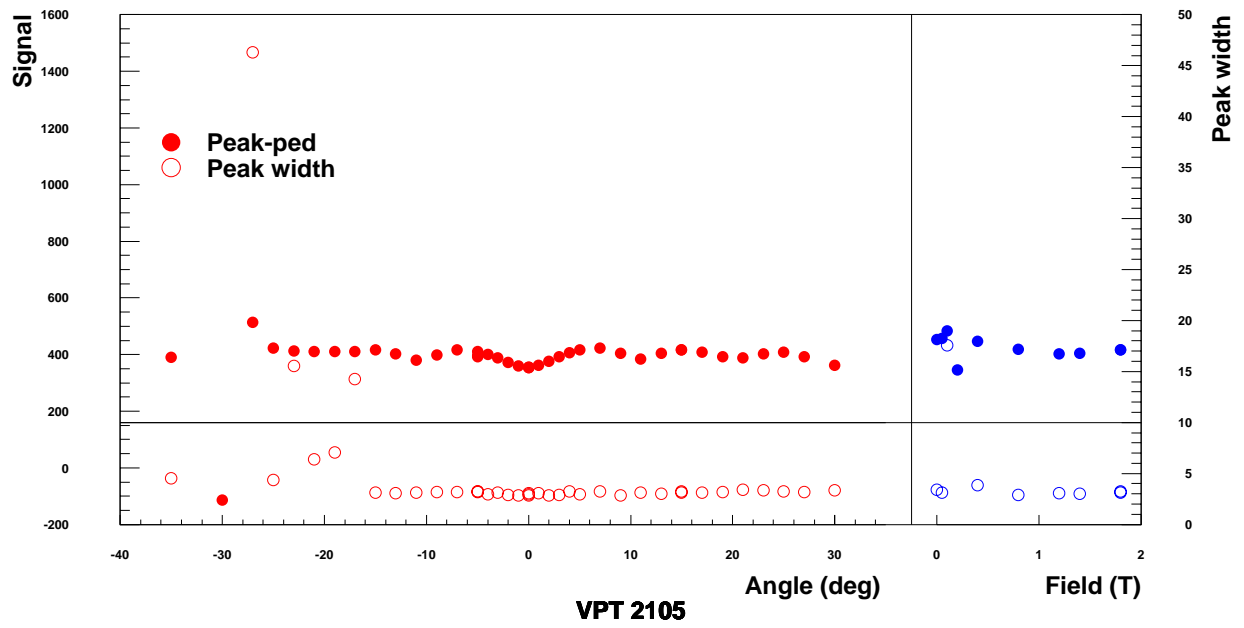
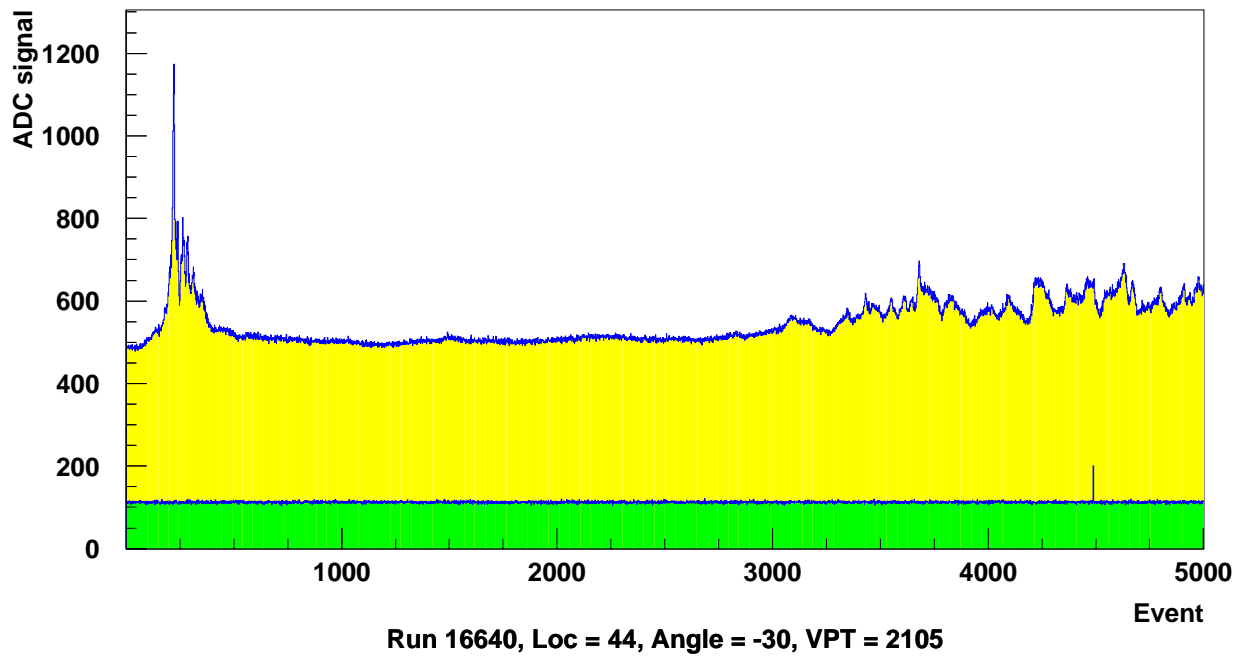


Figure 21. VPT 2105 - Standard measurement sequence



Run 16640, Loc = 44, Angle = -30, VPT = 2105  
Figure 22. VPT 2105 - raw data sequence at -30° to magnetic field

## 2.12 VPT 2174

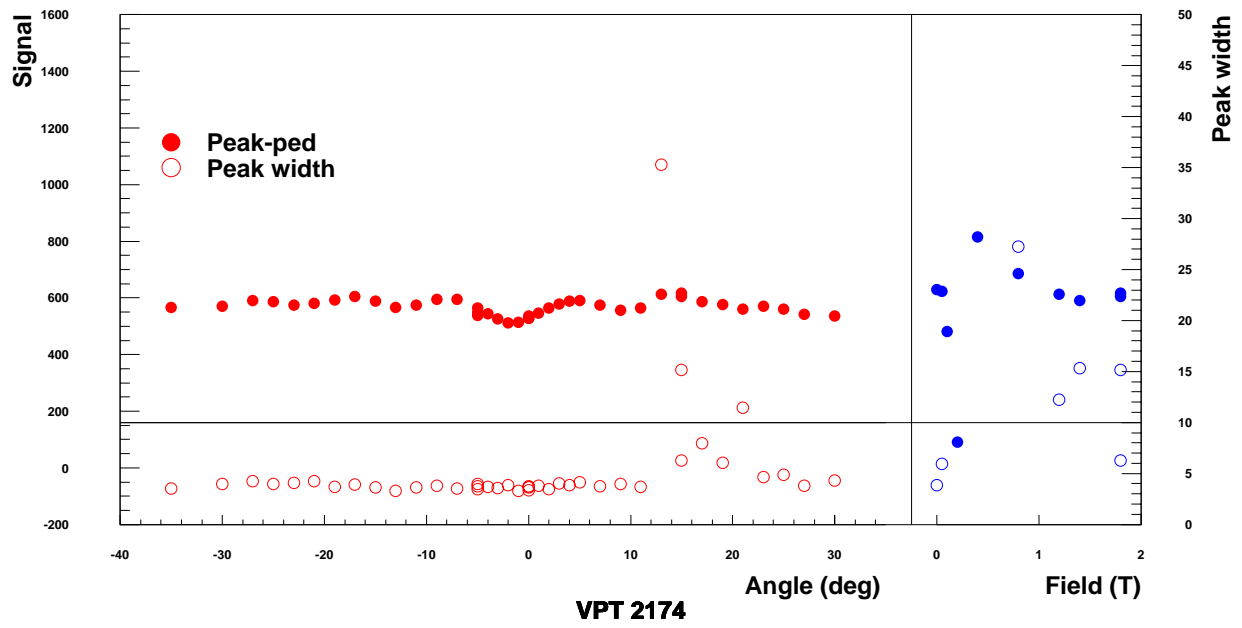


Figure 23. VPT 2174 - Standard measurement sequence

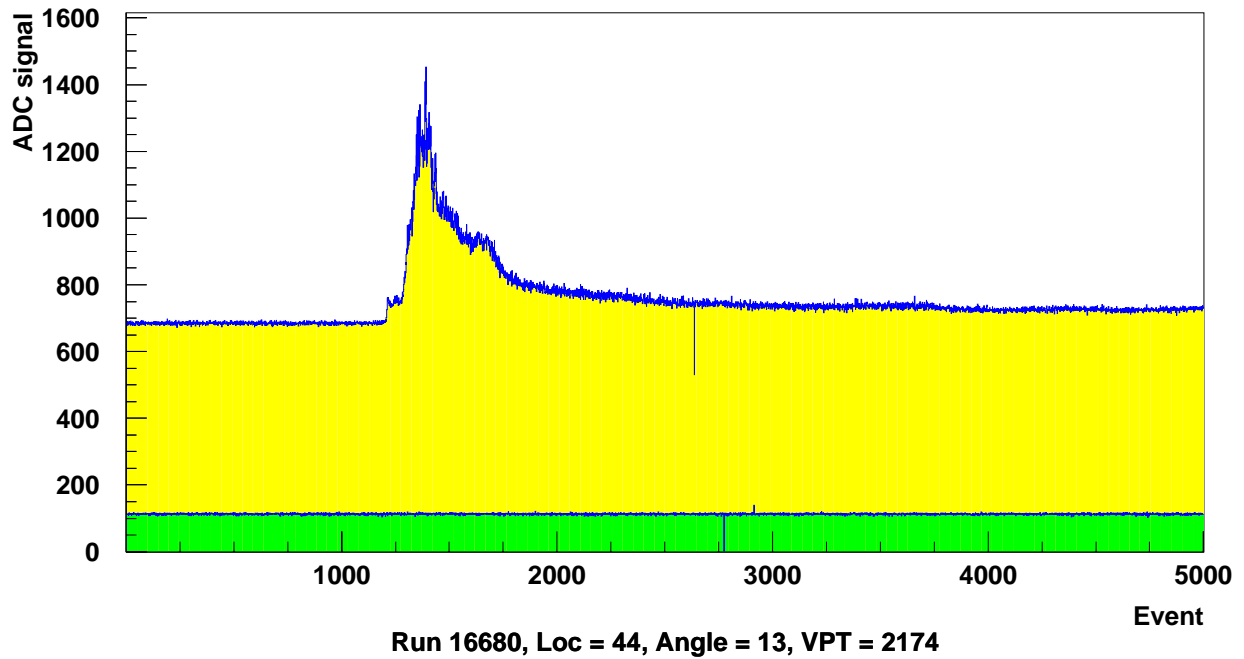


Figure 24. VPT 2174 - raw data sequence at  $13^\circ$  to magnetic field

### 2.13 VPT 2179

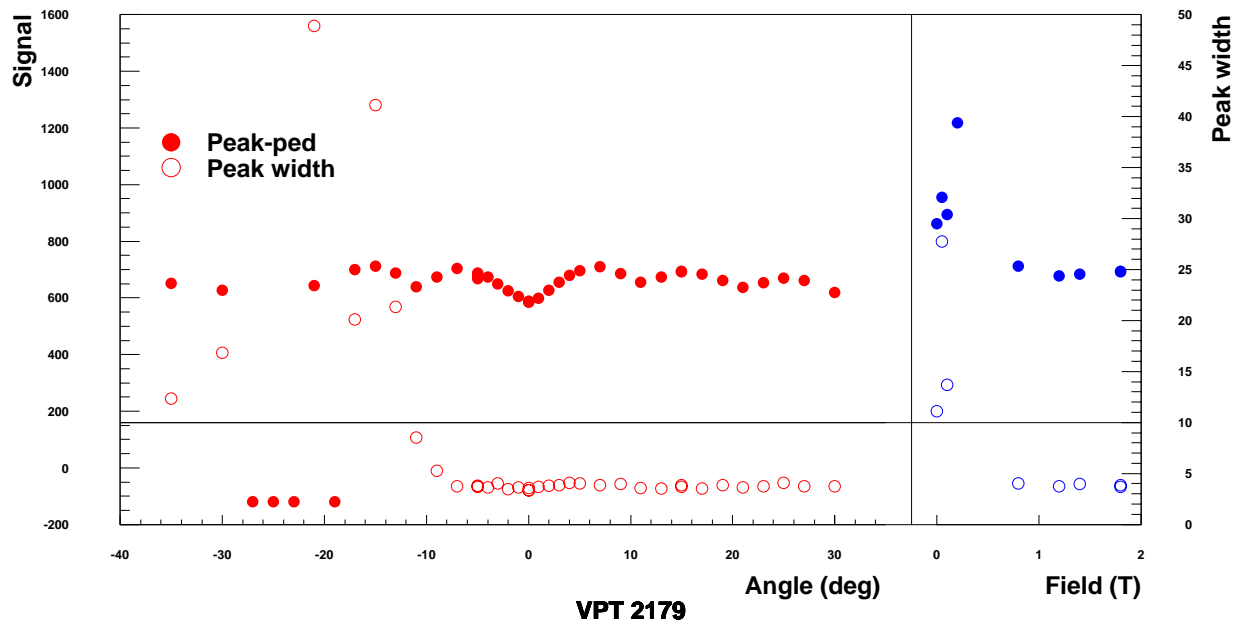


Figure 25. VPT 2179 - Standard measurement sequence

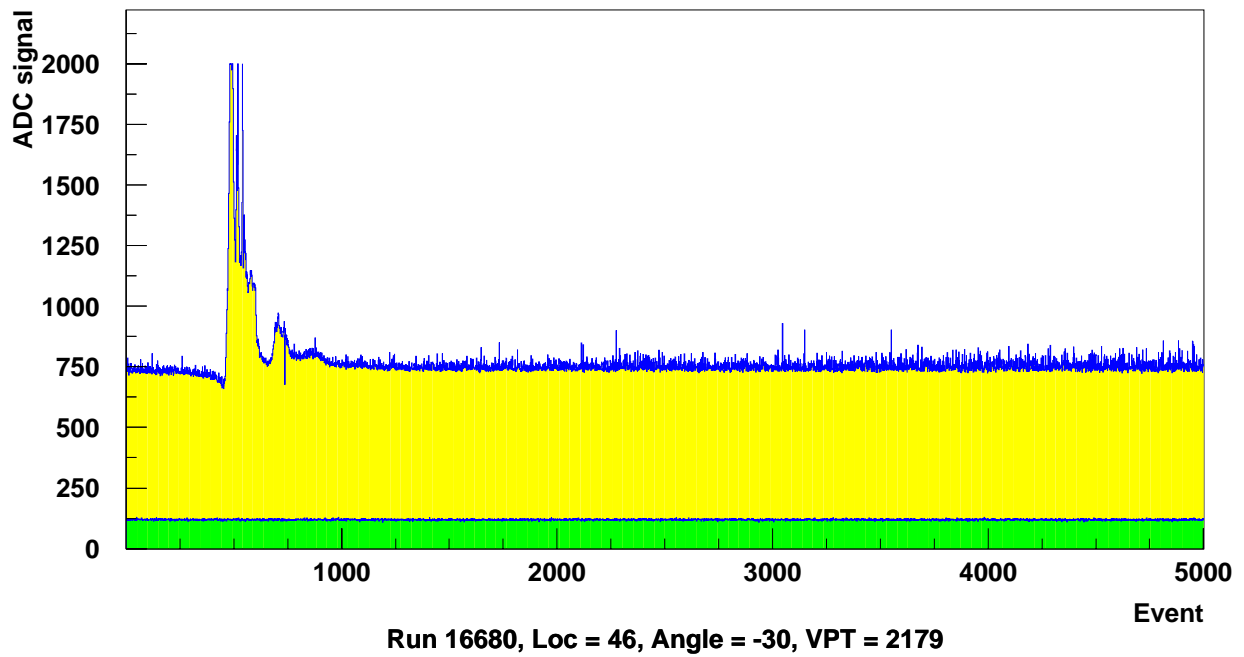


Figure 26. VPT 2179 - raw data sequence at  $-30^\circ$  to magnetic field

## 2.14 VPT 2256

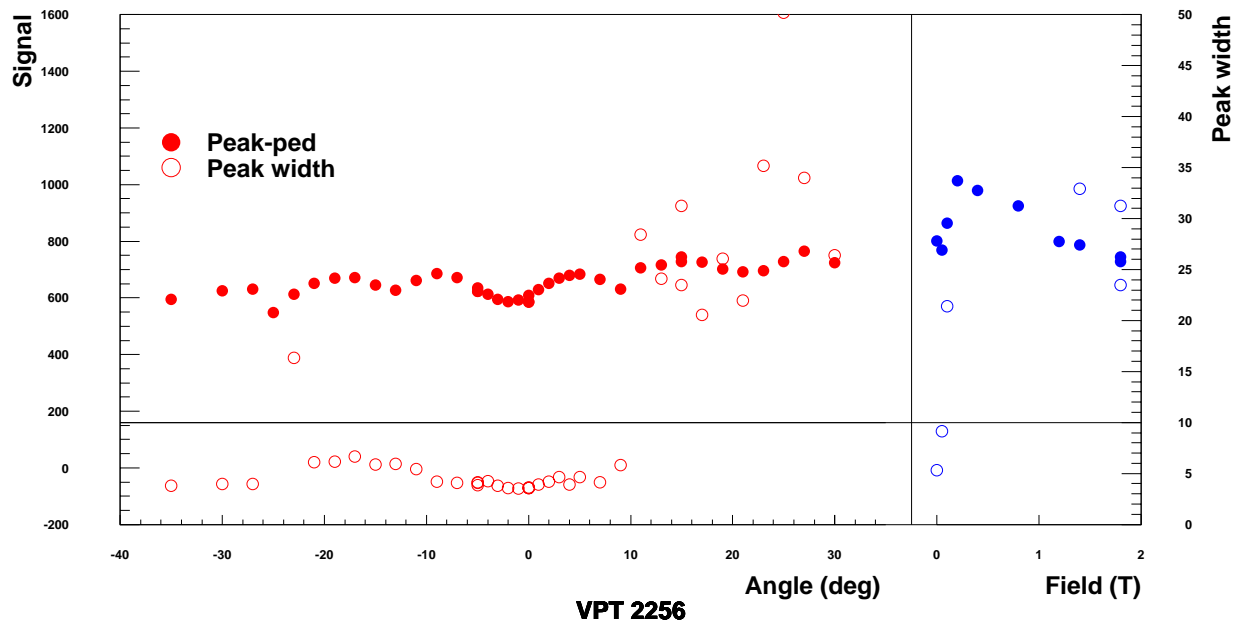
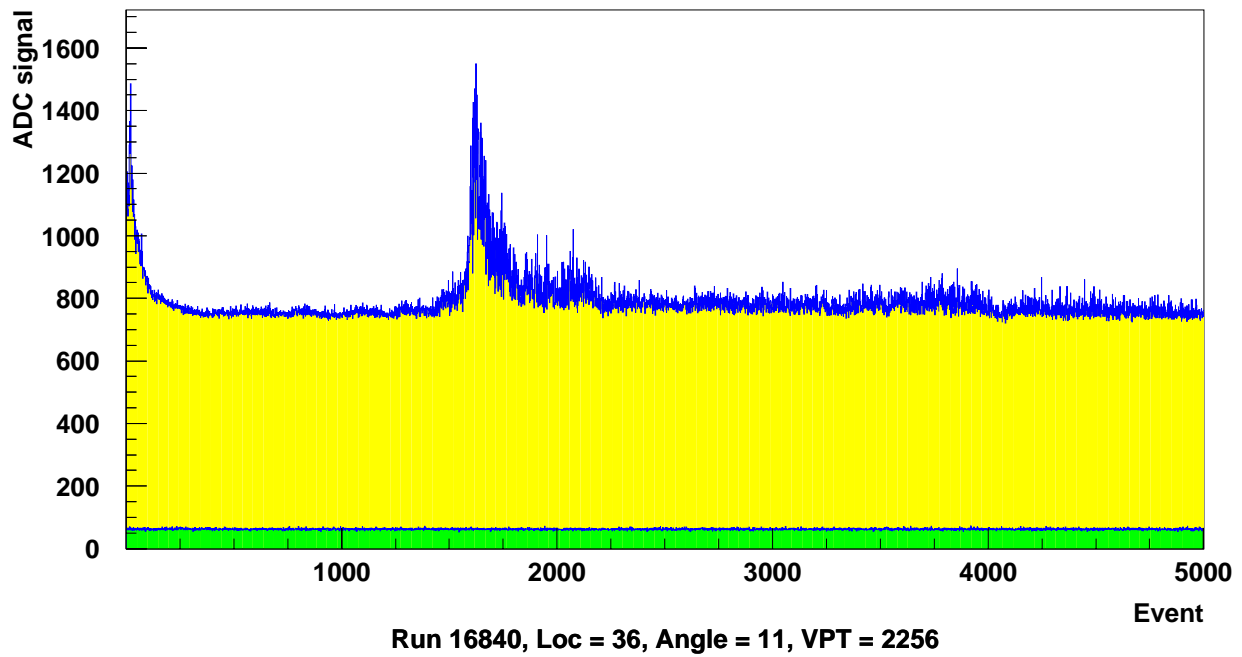


Figure 27. VPT 2256 - Standard measurement sequence



Run 16840, Loc = 36, Angle = 11, VPT = 2256  
Figure 28. VPT 2256 - raw data sequence at 11° to magnetic field

## 2.15 VPT 2304

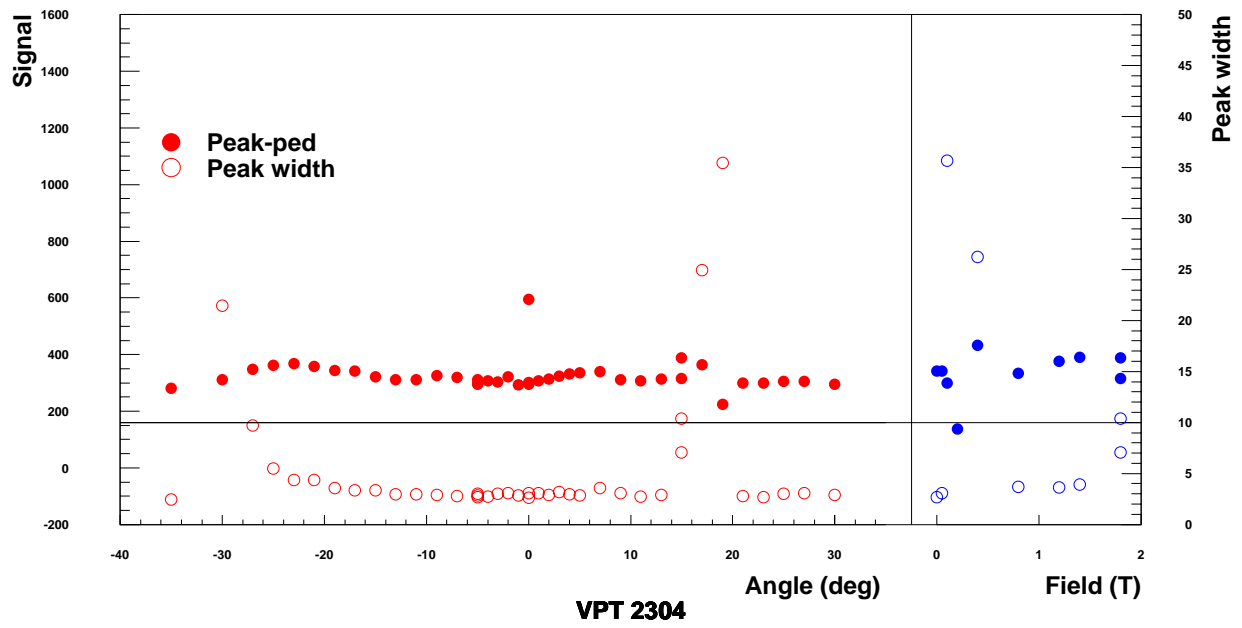


Figure 29. VPT 2304 - Standard measurement sequence

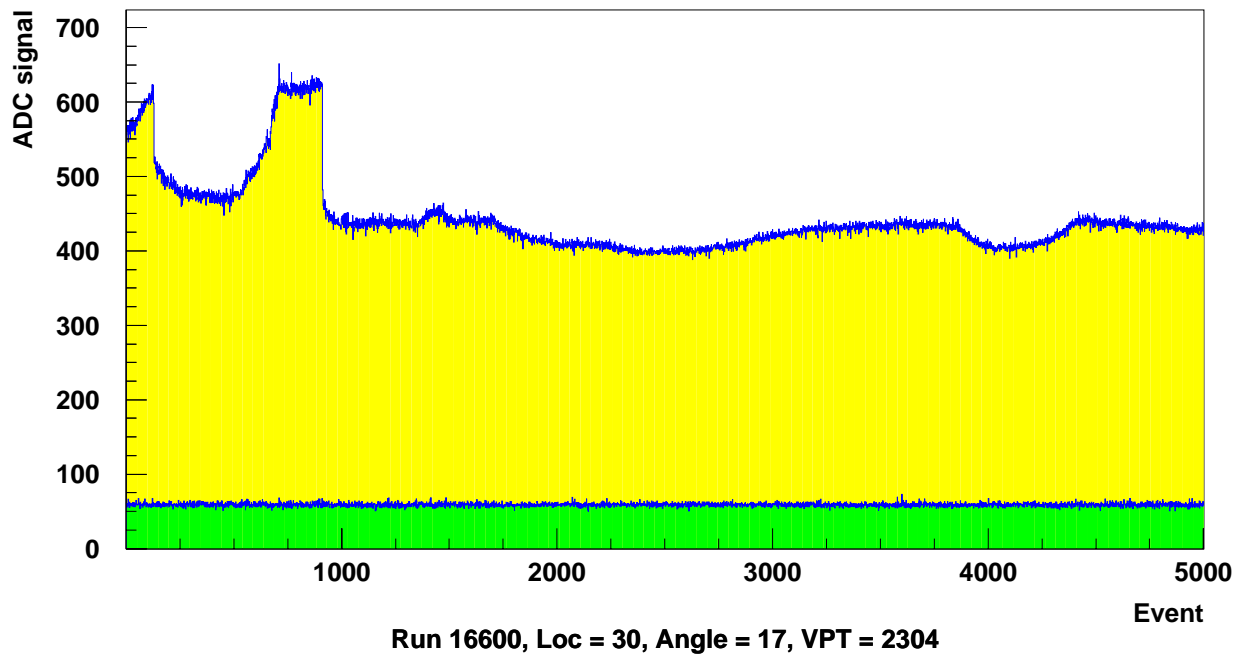


Figure 30. VPT 2304 - raw data sequence at 17° to magnetic field

## 2.16 VPT 2373

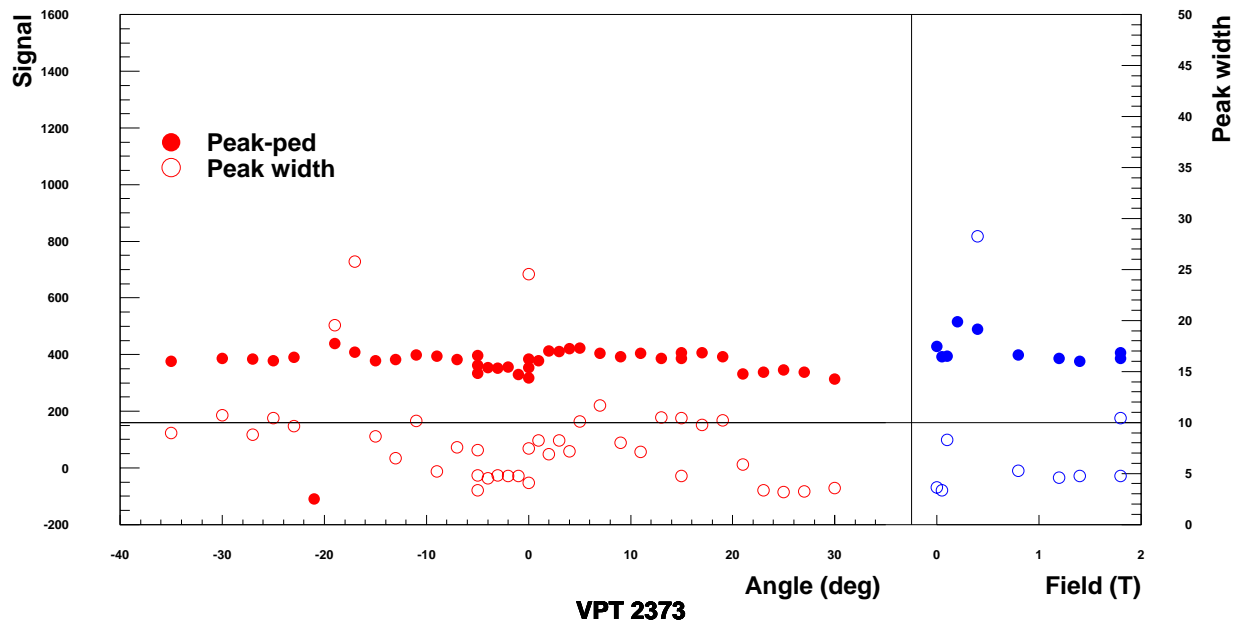


Figure 31. VPT 2373 - Standard measurement sequence

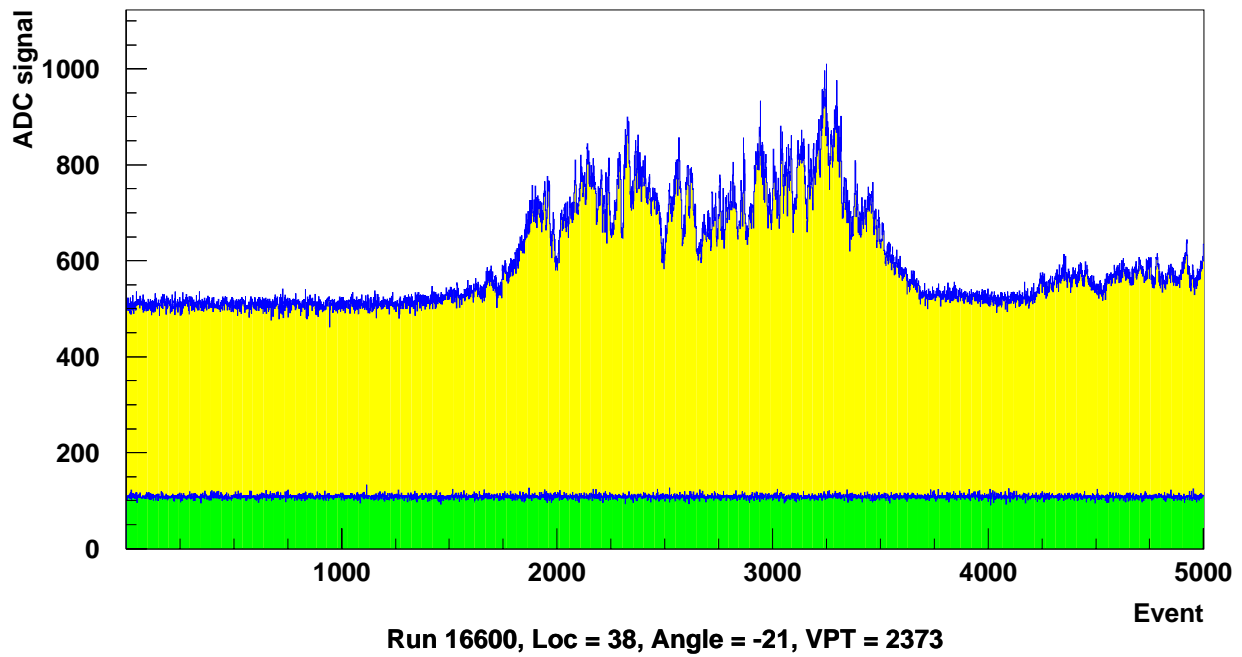


Figure 32. VPT 2373 - raw data sequence at  $-21^\circ$  to magnetic field

## 2.17 VPT 2395

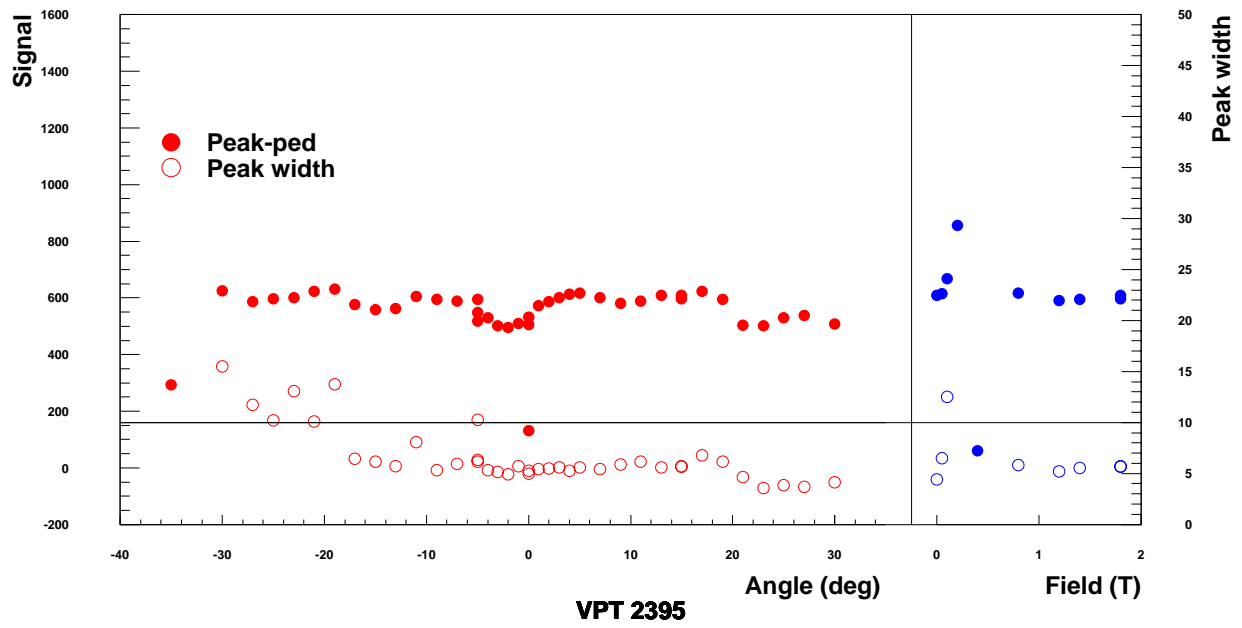
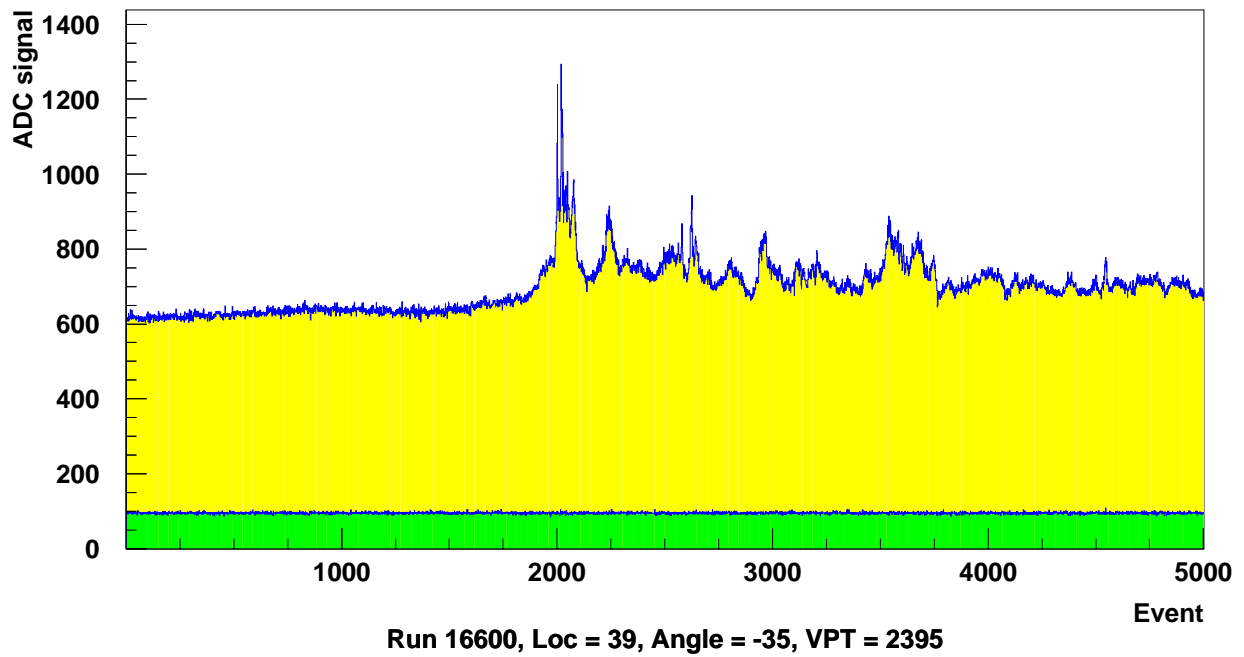


Figure 33. VPT 2395 - Standard measurement sequence



Run 16600, Loc = 39, Angle =  $-35^\circ$ , VPT = 2395  
 Figure 34. VPT 2395 - raw data sequence at  $-35^\circ$  to magnetic field

## 2.18 VPT 2413

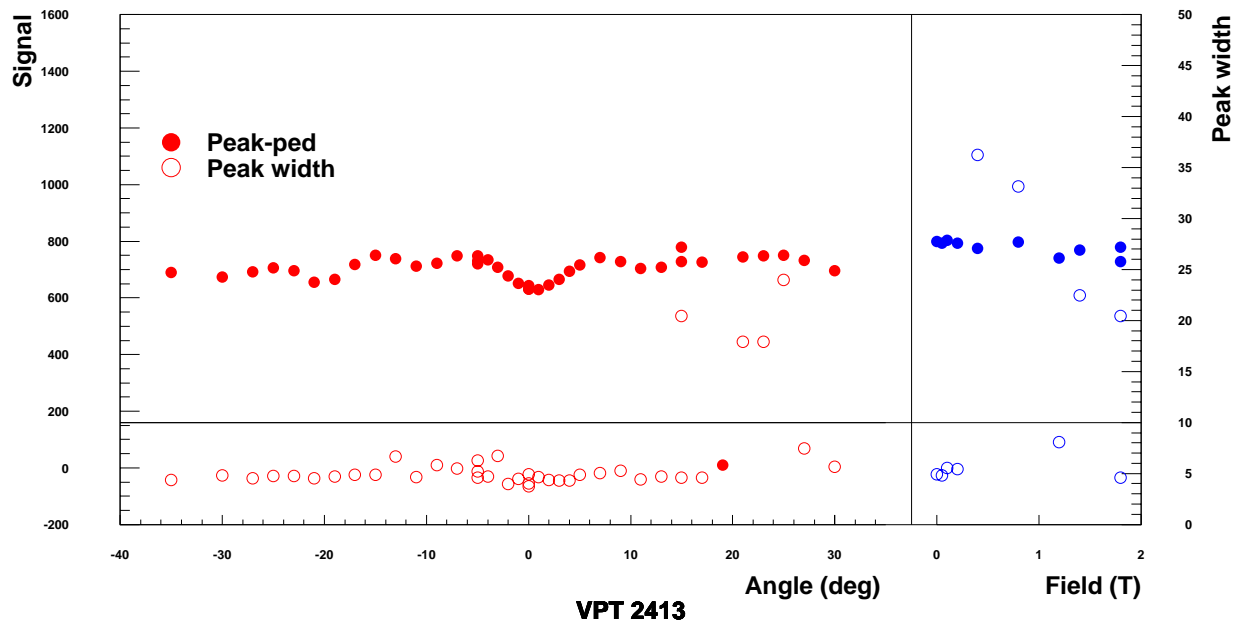


Figure 35. VPT 2413 - Standard measurement sequence

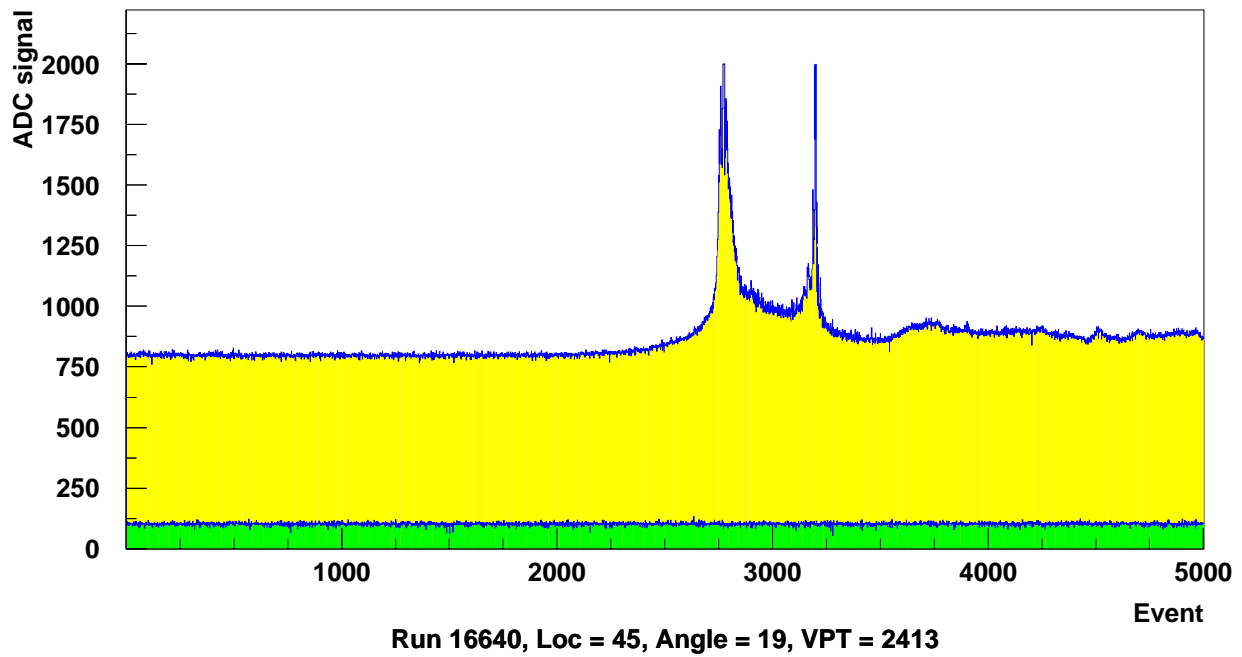


Figure 36. VPT 2413 - raw data sequence at  $19^\circ$  to magnetic field

## 2.19 VPT 2436

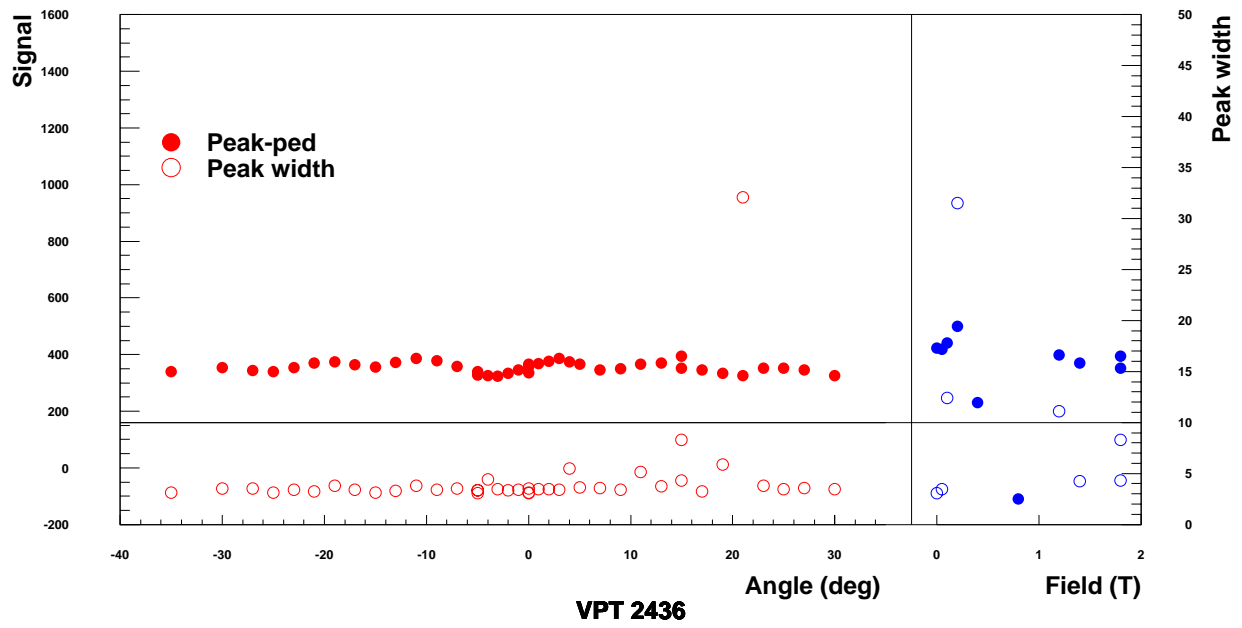


Figure 37. VPT 2436 - Standard measurement sequence

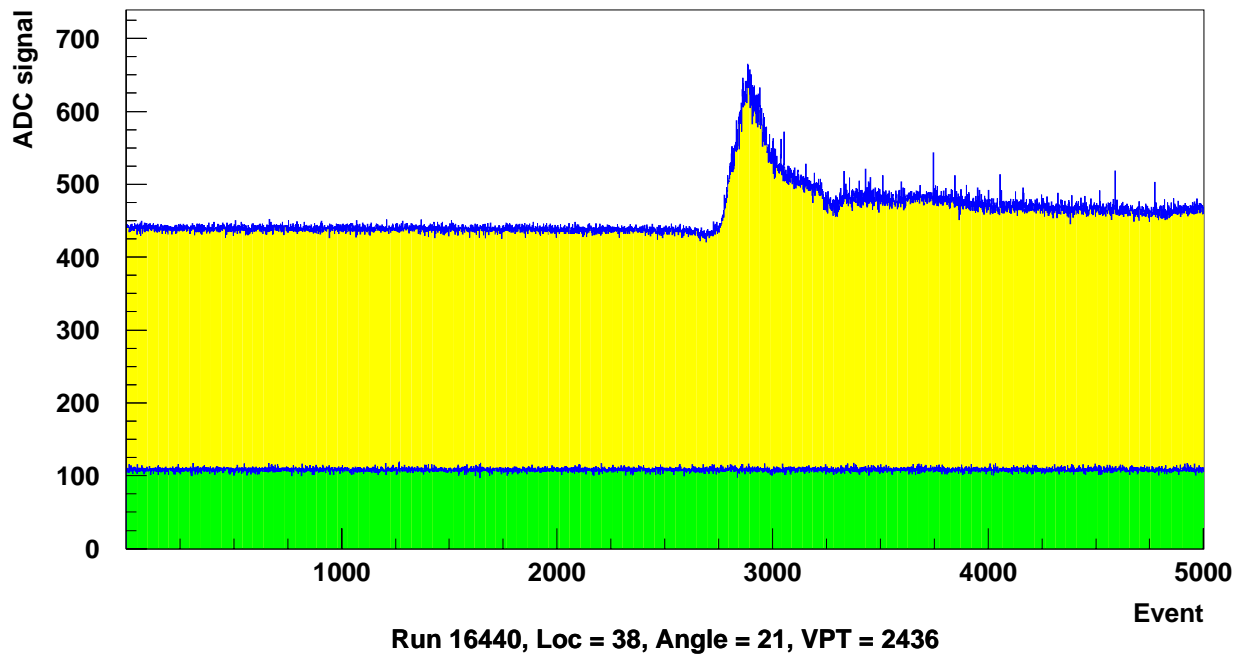


Figure 38. VPT 2436 - raw data sequence at 21° to magnetic field

## 2.20 VPT 2557

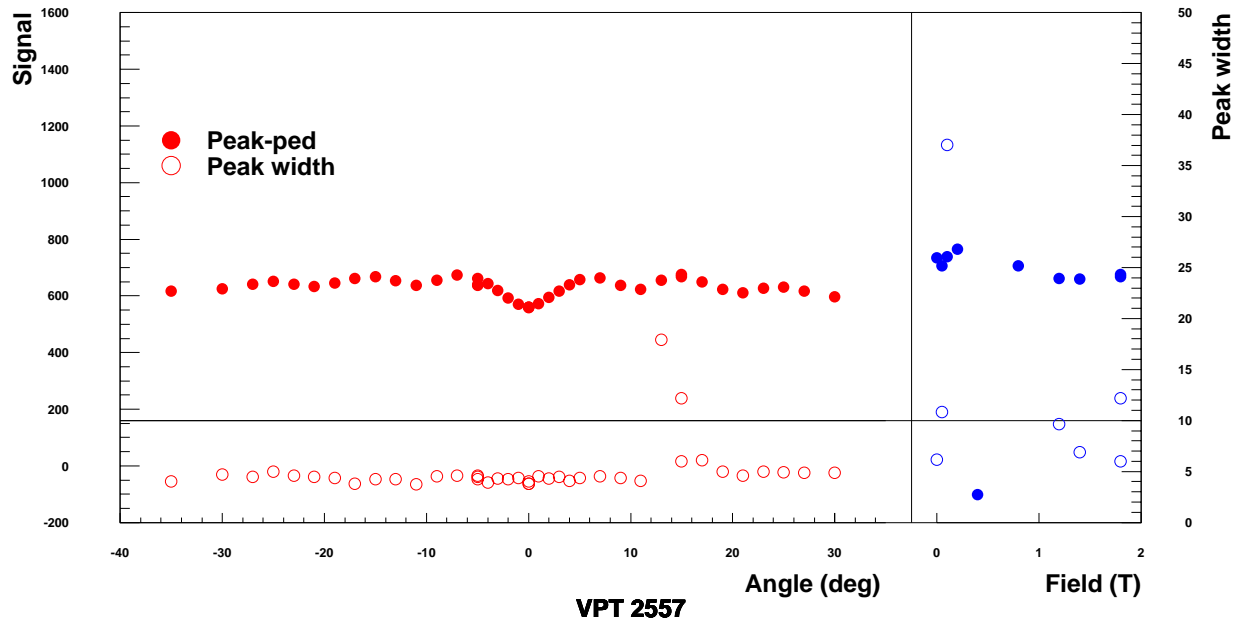


Figure 39. VPT 2557 - Standard measurement sequence

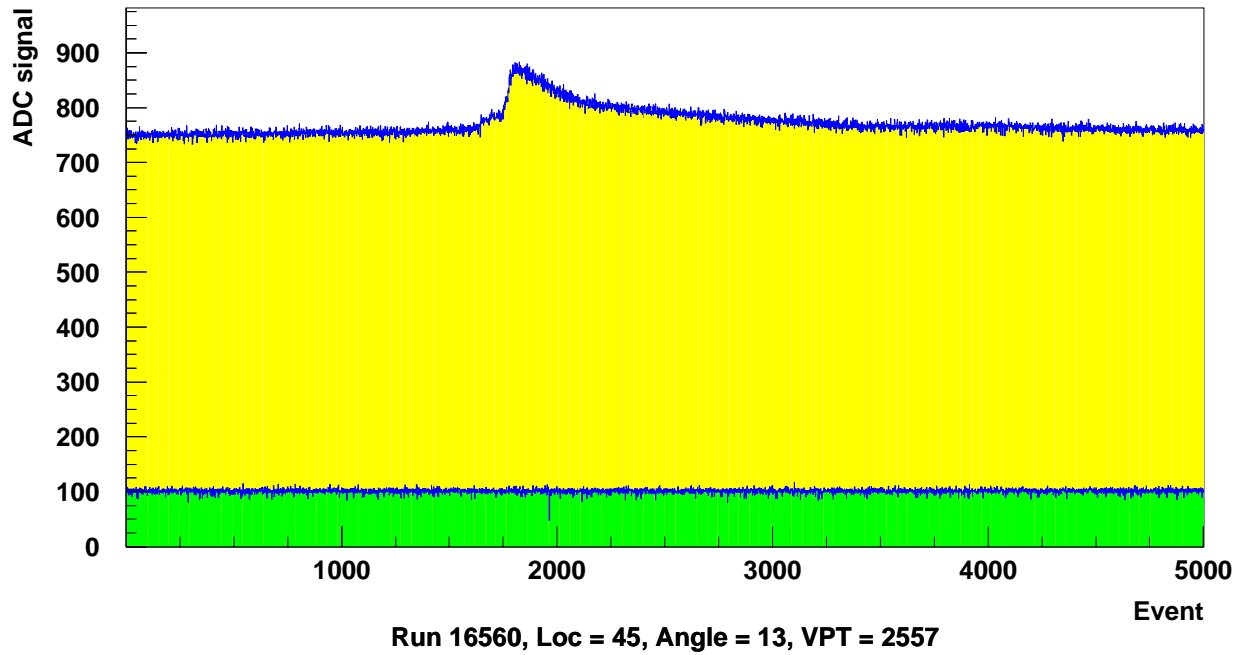


Figure 40. VPT 2557 - raw data sequence at 13° to magnetic field

## 2.21 VPT 2830

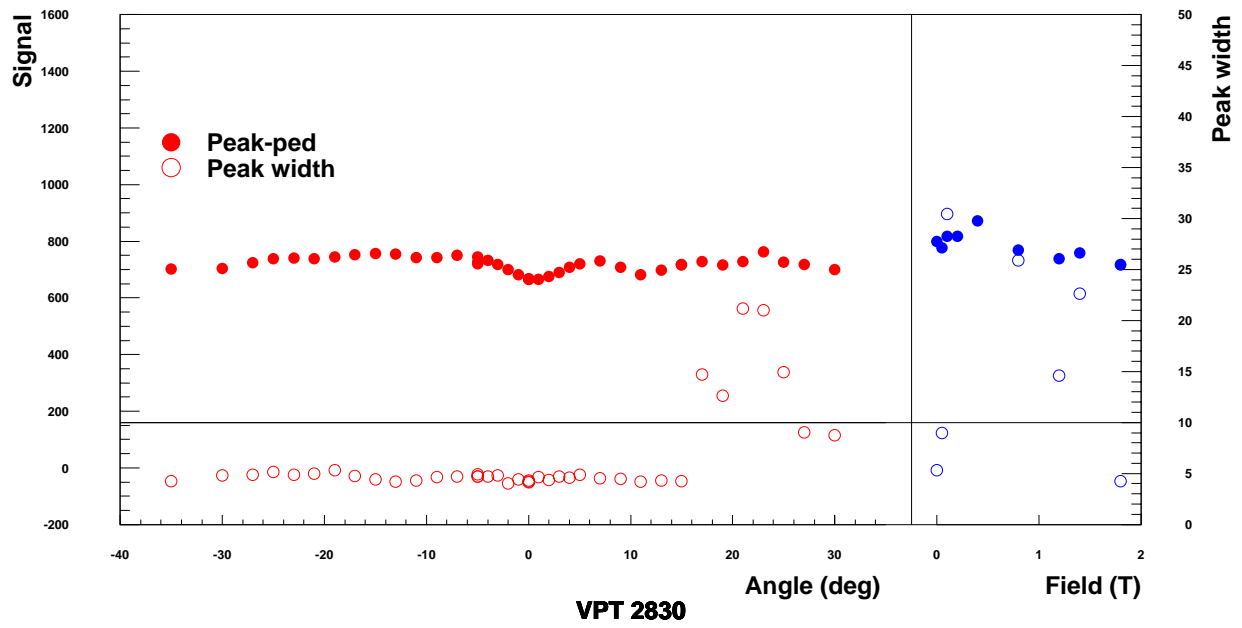


Figure 41. VPT 2830 - Standard measurement sequence

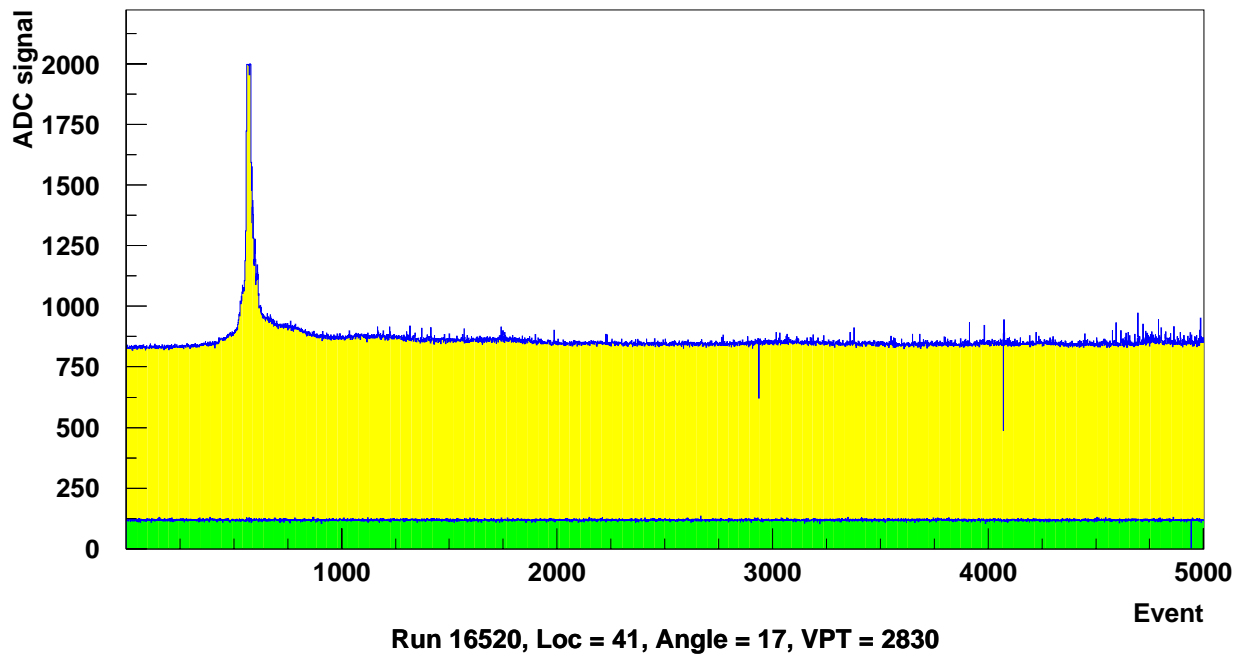


Figure 42. VPT 2830 - raw data sequence at 17° to magnetic field

## 2.22 VPT 3065

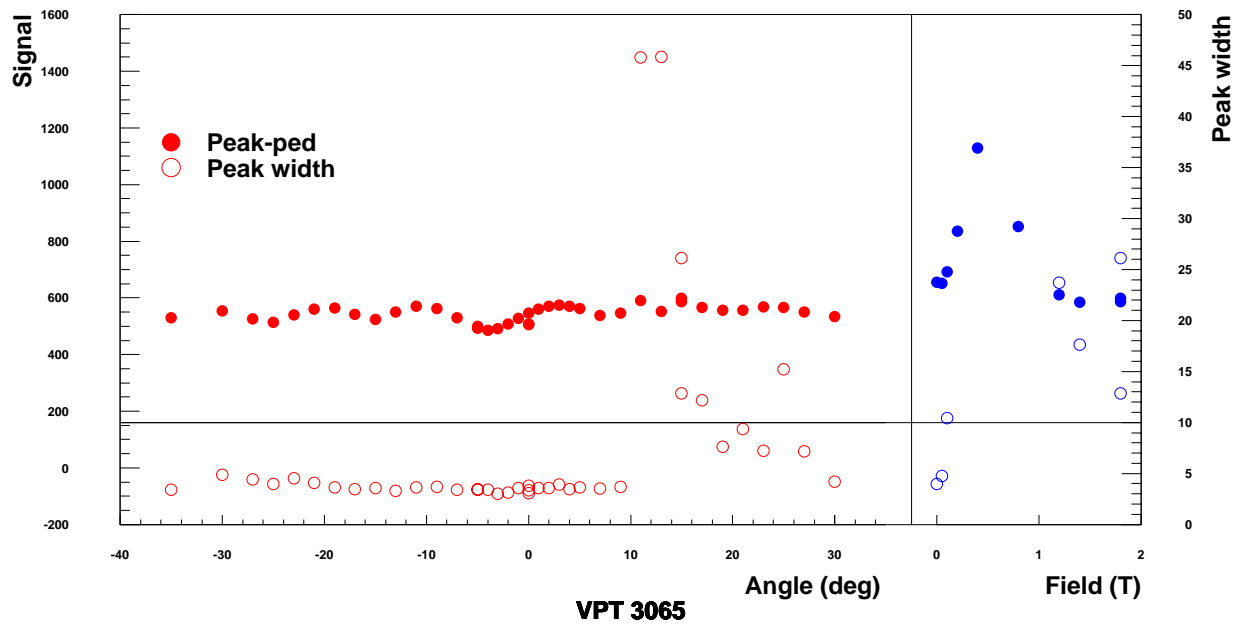


Figure 43. VPT 3065 - Standard measurement sequence

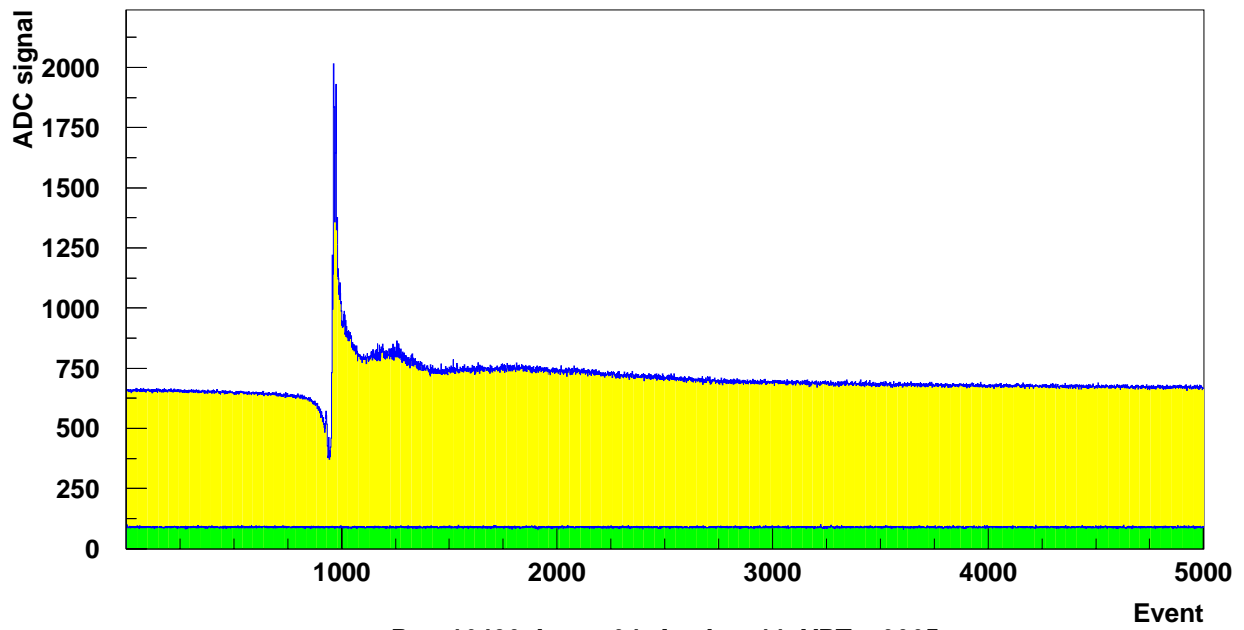


Figure 44. VPT 3065 - raw data sequence at 11° to magnetic field

## 2.23 VPT 3089

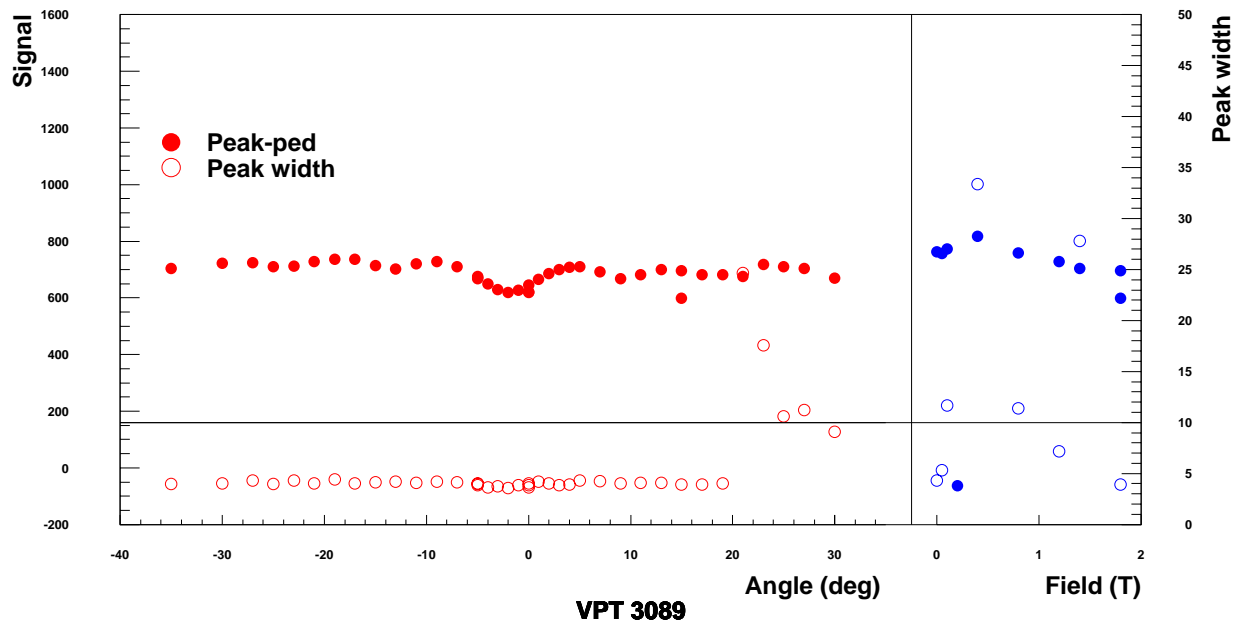


Figure 45. VPT 3089 - Standard measurement sequence

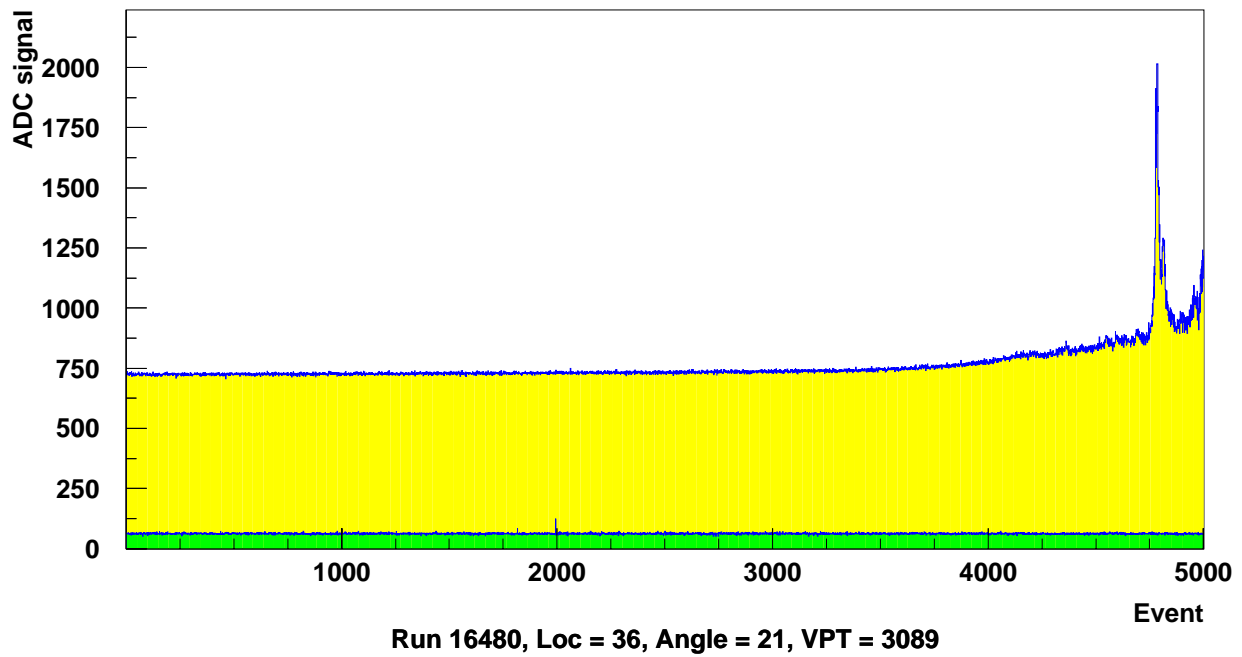


Figure 46. VPT 3089 - raw data sequence at 21° to magnetic field

## 3. REFERENCES

- [1] 'Observation of noise in production VPTs at 1.8T', B W Kennedy, 10 February 2003
- [2] 'Behaviour of production VPTs for the CMS Endcap Electromagnetic Calorimeter: VPTs 501-3200', B W Kennedy et al, 10 February 2003